# GEOLOGY AND MINERAL POTENTIAL OF THE ANTELOPE RANGE MINING DISTRICT, IRON COUNTY, UTAH

*By Michael A. Shubat and W. Skip McIntosh*

UTAH GEOLOGICAL AND MINERAL SURVEY
*a division of*
UTAH DEPARTMENT OF NATURAL RESOURCES
BULLETIN 125 1988

# UTAH GEOLOGICAL AND MINERAL SURVEY

606 Black Hawk Way
Salt Lake City, Utah 84108-1280

THE UTAH GEOLOGICAL AND MINERAL SURVEY is one of eight divisions in the Utah Department of Natural Resources. The UGMS inventories the geologic resources of Utah (including metallic, nonmetallic, energy, and ground-water sources); identifies the state's geologic and topographic hazards (including seismic, landslide, mudflow, lake level fluctuations, rockfalls, adverse soil conditions, high ground water); maps geology and studies the rock formations and their structural habitat; and provides information to decisionmakers at local, state, and federal levels.

THE UGMS is organized into five programs. Administration provides support to the programs. The Economic Geology Program undertakes studies to map mining districts, to monitor the brines of the Great Salt Lake, to identify coal, geothermal, uranium, petroleum and industrial minerals resources, and to develop computerized resource data bases. The Applied Geology Program responds to requests from local and state governmental entities for site investigations of critical facilities, documents, responds to and seeks to understand geologic hazards, and compiles geologic hazards information. The Geologic Mapping Program maps the bedrock and surficial geology of the state at a regional scale by county and at a more detailed scale by quadrangle.

THE INFORMATION PROGRAM distributes publications, answers inquiries from the public, and manages the UGMS Library. The UGMS Library is open to the public and contains many reference works on Utah geology and many unpublished documents about Utah geology by UGMS staff and others. The UGMS has begun several computer data bases with information on mineral and energy resources, geologic hazards, and bibliographic references. Most files are not available by direct access but can be obtained through the library.

THE UGMS PUBLISHES the results of its investigations in the form of maps, reports, and compilations of data that are accessible to the public. For future information on UGMS publications, contact the UGMS sales office, 606 Black Hawk Way, Salt Lake City, Utah 84108-1280.

# GEOLOGY AND MINERAL POTENTIAL OF THE ANTELOPE RANGE MINING DISTRICT, IRON COUNTY, UTAH

*By Michael A. Shubat and W. Skip McIntosh*

UTAH GEOLOGICAL AND MINERAL SURVEY
*a division of*
UTAH DEPARTMENT OF NATURAL RESOURCES
BULLETIN 125 1988

# CONTENTS

## ILLUSTRATIONS

# GEOLOGY AND MINERAL POTENTIAL OF THE ANTELOPE RANGE MINING DISTRICT, IRON COUNTY, UTAH

*By Michael A. Shubat[1] and W. Skip McIntosh[2]*

## ABSTRACT

THE Antelope Range mining district, located approximately 20 miles (32 km) west of Cedar City, Utah, contains many occurrences of epithermal, base and precious metals mineralized veins. Host rocks in the district range from limestone of the Carmel Formation through a sequence of Tertiary ash-flow tuffs. Neogene extensional faulting produced northwest-striking structures that host mineralized veins. The mineralization and hydrothermal alteration is approximately 8.5 Ma. Ore and gangue minerals show a paragenetic sequence that consists of an earlier base metals stage followed by a later silver sulfosalt stage. Maximum precious metal values from vein samples are 9 oz/ton silver and 0.22 oz/ton gold. Factor analysis results of geochemical data independently corroborate the paragenetic sequence. Both lateral and vertical geochemical zonations are inferred. Mineralization is interpreted to be the product of a boiling hydrothermal system induced by rhyolitic and dacitic volcanism. Potential exists for the discovery of silver-bearing epithermal vein deposits.

## INTRODUCTION

The Antelope Range mining district, located approximately 20 miles (32 km) west of Cedar City, lies largely within the west-central portion of the Antelope Range. Flanking physiographic features include the Escalante Desert to the west and north, Neck of the Desert (part of the Escalante Desert) to the east, and a series of isolated peaks and low hills rising to the Pine Valley Mountains to the south (figure 1). The Antelope Range has a steep western range-front with approximately 2000 feet (610 m) of relief and a maximum elevation of 7416 feet (2262 m). Pinyons and junipers cover the crest and gently sloping eastern flank of the range. Two major canyons, Chloride and Bullion Canyons, dissect the range. The town of Newcastle lies approximately 6 miles (9 km) southwest of the center of the range and the Iron Springs district lies to the east. Numerous dirt roads departing from Highway 56, including the Joel Spring Canyon road and the Antelope road (figure 1), provide access. The district lies largely within the Silver Peak quadrangle (1:24,000 scale).

[1]Geologist, Utah Geological and Mineral Survey

[2]Colorado State University, Fort Collins, Colorado

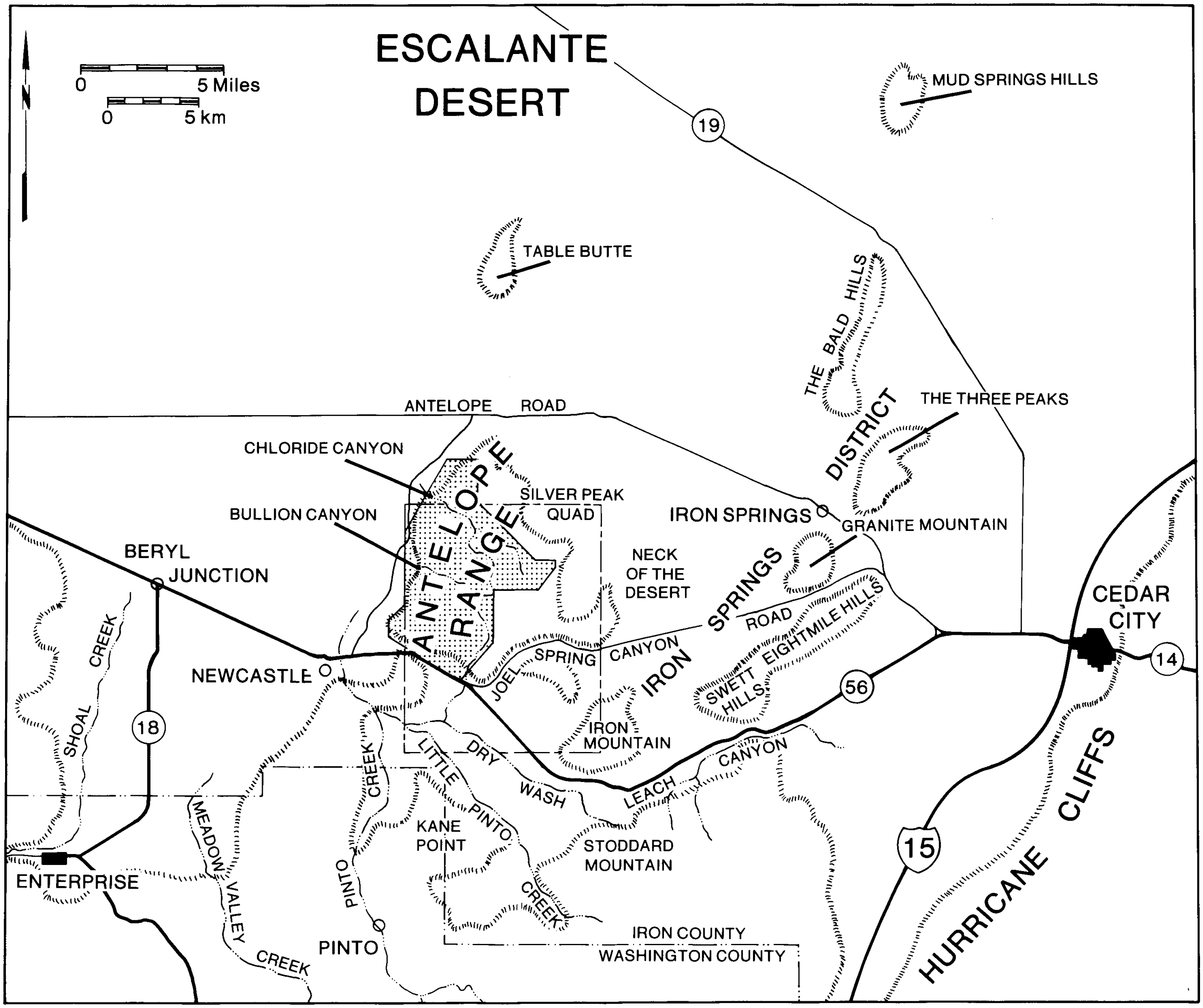


**Figure 1.** Location map of the Antelope Range mining district (stippled) and the Silver Peak quadrangle (dashed).

## MINING AND EXPLORATION HISTORY

Early historic references to the Antelope Range district are sparse, but prospecting apparently began in the 1870s. In 1885, a brief mention of the district was made in the U.S. 10th Census (Huntley, 1885). At this time the district was part of the Pinto district, however, during the period from 1873 to 1875 the Antelope Range district was formally recognized as the Silver Belt district. Huntley visited the district in July, 1880 and made the following observations:

> It is located north of the Pinto district, and contained at the time of the writer's visit 60 locations. The ore is quartzite, with some copper stain and lead, and assays from \$40 to \$60 silver per ton. The veins are from 2 to 4 feet wide. The developments are limited.

In 1890 and in 1905, a Mr. Blair conducted small-scale mining (Fournier, unpublished report, 1978). Mr. Blair sunk two shafts and dug prospect pits in the southern part of the district ("Blair area," plate 2). During this development, an undetermined amount of ore was sent by horse or donkey cart to the Silver Reef district for processing. In 1901, an article on the Blair area appeared in the Salt Lake Mining Review (Anonymous, 1901), which gave the following optimistic report:

> It is learned that the Pinto Gold and Copper Company of Cedar City has given a 30 day option on its group of 9 claims in Pinto Iron district to W.J. Dooley. This property was formerly known as the Blair Mine and was owned several years ago by a Logan Company. The group covers a very large and strong vein which carries excellent values in silver, gold, and copper. When the mine was first worked it figured on the shipping list to a limited extent. It is a valuable proposition and if the option is not taken up during its life, which terminates on June 15th, it is the intention of the owner to begin work at once on its development.

Another article in the Salt Lake Mining Review (Anonymous, 1913) reported that the Silver Chloride Mining Company, under the management of a Mr. Rickards, drove a 150-foot tunnel to intersect "the main ledge of the property." The location of this tunnel was not given.

Most exploration in the district since the 1950s focused on the Blair area. Heber Holt (of Enterprise, Utah) located claims in the Blair area in the late 1950s and an optionee (Richard Wyman of St. George, Utah) drilled two holes, which apparently did not encounter significant ores. In 1960, three persons (Wyant, Kundert, and Davenport) conducted a mapping and sampling program. In the late 1960s, Cotter Corporation (of Golden, Colorado) drilled a hole 1001 feet (305 m) deep.

More intensive exploration of the district began after 1970. In 1971, Ranchers Exploration, Inc. (of Albuquerque, New Mexico) conducted an exploration program consisting of mapping and sampling in the Blair area. Ranchers drilled one hole that reportedly intersected a vein containing 45 percent carbonate. Newmont Mining later conducted a soil sampling program across the area but dropped their holdings in 1973. After Newmont, Geologic Resources, Inc. of Albuquerque acquired a ten-year lease option on the Blair area and conducted a mapping, sampling, and drilling program. Geologic Resources, Inc. noted an inverse relationship between silver grades and the calcite content of veins, and they reported a maximum silver value of 3.94 oz/ton from drill core.

Exploration by Houston Oil and Minerals Company (now Tenneco Minerals) began in 1976, and consisted of extensive mapping, geochemical sampling, and drilling. This work covered the southern two-thirds of the district. Houston drilled thirteen holes in three separate areas. A final report on exploration activities by R. Fournier (unpublished report, 1978) was made available to the authors along with supporting data. Work by Houston terminated in 1979. Ranchers Exploration conducted limited exploration in the northern portion of the district in the early 1980s. The Homestake Mining Company conducted the most recent exploration, commencing about 1980. Their mapping and sampling focused on the Bullion Canyon area.

### PREVIOUS WORK

Published information on the Antelope Range district is limited to the previously cited references by Huntley (1885) and two anonymous authors in the Salt Lake Mining Review. Much work, however, was done in the nearby Iron Springs district where stratigraphic and structural concepts pertinent to the Antelope Range district were first defined.

Pioneering efforts in the Iron Springs district by Leith and Harder (1908) consisted of geologic mapping. Large-scale mining began in 1923, and during World War II the district supplied much of the iron ore for western U.S. steel plants. Strategic concerns during the war prompted the U.S. Geological Survey to initiate geological investigations in the district, led by J. Hoover Mackin. An intensive period of study ensued that resulted in many publications on the structure, stratigraphy, and economic geology of the region. Key publications on stratigraphy include those by Williams (1967), Cook (1965), Anderson and others (1975), Blank (1959), and Mackin (1960). Mackin (1947; 1960) outlined the structural relations in the Iron Springs district. Several authors discussed the economic geology of the district (Mackin, 1947; 1968; Lewis, 1958; Ratté, 1963; Bullock, 1970; 1973; and Rowley and Barker, 1978).

Literature of regional scope pertaining to the Antelope Range district includes papers by Rowley and others (1979) and Steven and Morris (1984), which provide an excellent account of the geologic setting. Gravity surveys by Pe and Cook (1980), in the Escalante Desert, and Cook and Hardman (1967) cover much of the Cedar City 2° quadrangle. Blank and Mackin (1967) conducted aeromagnetic studies in the region. Clement (1980) conducted an investigation of the geothermal potential of the Escalante Desert and Newcastle KGRA.

## GEOLOGY

### REGIONAL SETTING

The Antelope Range district lies at or near the intersection of several regional features, including the Basin and Range-Colorado Plateau transition zone, the "Iron Axis" (Tobey, 1977), the Timpahute lineament (Ekren and others, 1976), the Delamar-Iron Springs mineral belt (Shawe and Stewart, 1976), the eastern margin of the Sevier thrust belt (Armstrong, 1968), and the Intermountain seismic belt (Smith, 1978). Coincidence of these features supports the concept that the district lies within a long-lived volcano-tectonic boundary active since the Late Cretaceous and possibly earlier.

Events recorded by the stratigraphy of the district include a Middle to Late Jurassic marine invasion (Carmel Formation), erosion of the Late Cretaceous Sevier orogenic highland (Iron Springs Formation), Oligocene and early Miocene ash-flow tuff volcanism (Isom Formation and Quichapa Group), and late Tertiary bimodal volcanism (local rhyolite and dacite flows). Structural events include Late Cretaceous thrusting during the Sevier orogeny and Neogene extensional faulting. A bimodal volcanic suite replaced Oligocene to middle Miocene calc-alkaline volcanism in the region about 21 Ma (Rowley and others, 1979; Steven and Morris, 1984). The shift to bimodal volcanism coincided with the onset of extensional tectonics.

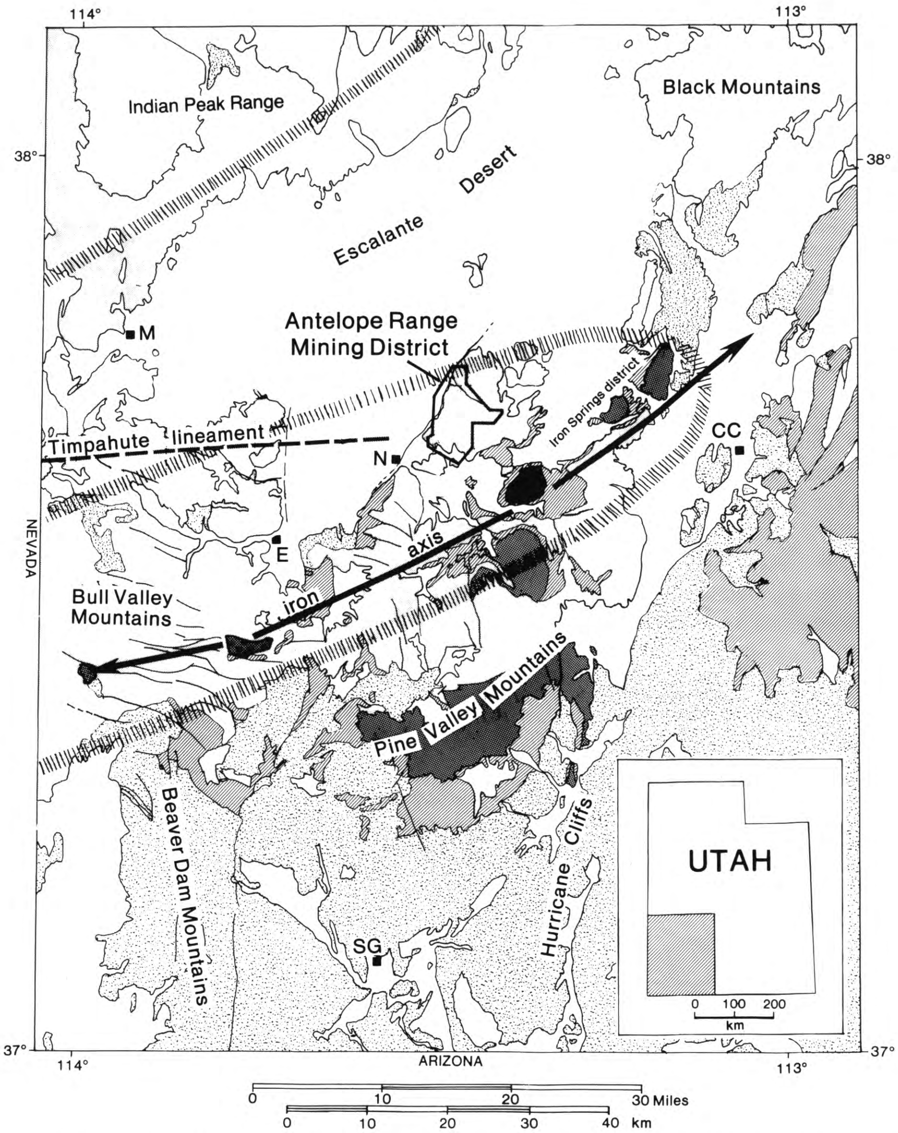


**Figure 2.** General geology and structural features of southwestern Utah. Light shaded areas include Tertiary lavas, ash-flow tuffs, and volcaniclastic units. Diagonal line shading includes both Claron (Eocene-Oligocene) and Iron Springs (Cretaceous) Formations. Dark shaded areas are Miocene plutons; mineralized plutons lie along the iron axis. Stippled areas include all other rocks from Precambrian through Mesozoic and some Quaternary basalts. Hachured lines enclose the Pioche mineral belt (north) and the Delamar-Iron Springs mineral belt (south). M, Modena; E, Enterprise; N, Newcastle; CC, Cedar City; SG, St. George. Structural features from Rowley and others (1979) and Tobey (1977).

Of interest in the area is the mode of extensional faulting active during the Neogene. Surficially, the structures appear to conform to the bipartite scheme of Zoback and others (1981) who proposed that pre-basin-range extension (20 to 10 Ma) preceded basin-range extension 10 Ma to present), with each period marked by unique structural styles and paleostress orientations. Other workers, however, argue that no such division of age or structural styles can be made and that low-angle detachment faulting may have produced much of the observed deformation (Wernicke, 1981; 1985; in press).

## STRATIGRAPHY

### Mesozoic

**Carmel Formation**—Mid-Jurassic rocks of the Carmel Formation, exposed in the Bullion Canyon area (plate 1) are the oldest rocks in the district (figure 3). The Homestake Limestone Member (Jch, plate 1), a light- to medium-gray, massive to thick-bedded limestone, has a minimum thickness of 160 feet (50 m). The unit is present throughout the nearby Iron Springs district and is the primary host for replacement iron ore deposits (Rowley and Barker, 1978). Locally exposed siltstone and sandstone (including a distinctive maroon, spotted sandstone bed) overlie the Homestake Limestone Member and correlate with the banded member (Jcb) of the Carmel Formation (Mackin and others, 1976).

**Iron Springs Formation**—Upper Cretaceous rocks of the Iron Springs Formation (Kis) underlie much of the lower Bullion Canyon area (plate 1). The formation consists of thin- to thick-bedded continental sandstone with lesser amounts of shale, conglomerate, and limestone. Johnson (1983) proposed a fluvial, braided stream depositional environment for the formation. The unit attains a maximum thickness of 3600 feet (1100 m) in the district. An unconformity at the base of the Iron Springs Formation marks a hiatus of as much as 80 Ma. A discontinuous, light-colored, quartzite cobble-rich conglomerate lies at the base of the Iron Springs Formation and may correlate with the Dakota Conglomerate (Hintze, 1986).

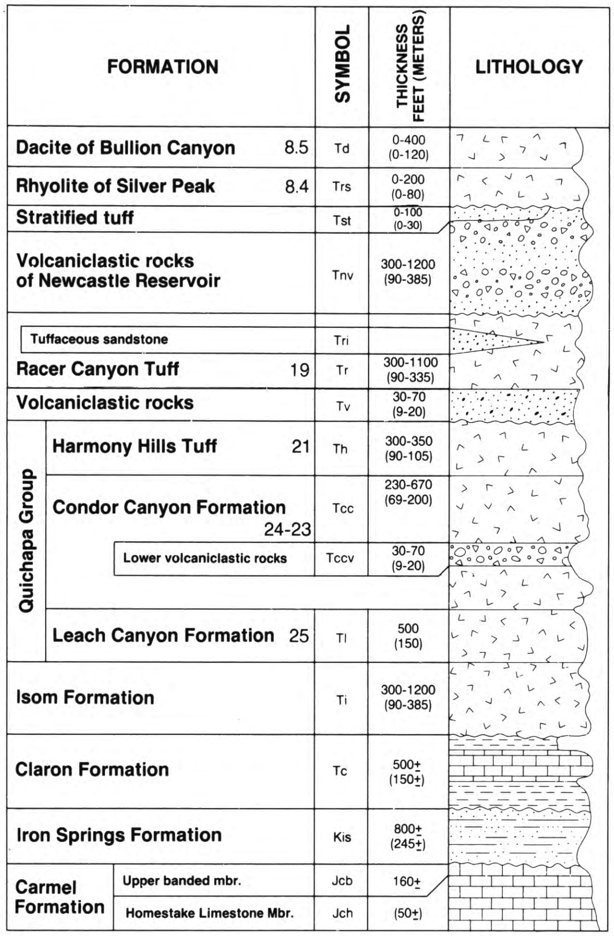


**Figure 3.** Columnar stratigraphic section of the Antelope Range mining district. K-Ar ages of dated volcanic units shown in left column in Ma. Thicknesses given in feet and meters (in parentheses). Wavy lines mark unconformities.

## Cenozoic

**Claron Formation**—Paleocene to Oligocene rocks of the Claron Formation (Tc) paraconformably overlie the Iron Springs Formation. Fluvial and lacustrine shale, sandstone, limestone, and conglomerate comprise the formation. In general, red clastic rocks dominate in the lower half of the formation and light-gray limestones in the upper half. A maximum thickness of 950 feet (290 m) occurs in the Bullion Canyon area.

**Isom Formation**—The Isom Formation (Ti) marks the onset of ash-flow tuff volcanism in the Antelope Range district. Originally defined by Mackin (1960) in the Iron Springs district, the formation consists of two regional ash-flow tuff sheets, the lower Baldhills Member (Tib) and upper Hole-in-the-Wall Tuff Member (Tih), and locally intercalated lavas and sedimentary rocks. Both members are dark colored, sparsely porphyritic (less than 10 percent phenocrysts composed of plagioclase, minor clinopyroxene, and magnetite), and densely welded. Stretched vesicles (as much as 1 foot in length) and flattened light gray lenticules (less than 2 feet long) characterize the unit. Shubat and Siders (1988) and McIntosh (1987) give more complete descriptions of this and other volcanic units in the area. A maximum thickness of the combined members of over 1200 feet (360 m) occurs near the mouth of Chloride Canyon, much thicker than reported for the Iron Springs district. This northwestward thickening may reflect the presence of a source caldera or vent area beneath the Escalante Desert (Best, 1986, figure 6, p. 83). K-Ar methods yielded a date of 26 Ma for the formation (Rowley and others, 1979; new decay constants applied).

**Quichapa Group**—A sequence of widely distributed ash-flow tuffs, the Quichapa Group, overlies the Isom Formation. Mackin (1954; 1960) and Cook (1957) originally defined the units and Williams (1967) studied the tuffs in detail. Source calderas for the Quichapa tuffs may lie within the Caliente depression (Ekren and others, 1977).

Immediately overlying the Isom Formation is the Leach Canyon Tuff (Tl) of the Quichapa Group. Two members, the lower Narrows Member and upper Table Butte Member, comprise the formation. Both members are rhyolitic vitric-crystal to crystal-vitric ash-flow tuffs containing conspicuous red lithic clasts. Both are moderately welded and have a light-colored matrix. Crystal contents of the tuffs range between 20 and 30 percent, consisting of plagioclase, quartz, sanidine, minor biotite, Fe-Ti oxides, hornblende and sphene. Fresh plagioclase is rare within the district. Where the tuffs are strongly altered, modal analyses were required to differentiate the Leach Canyon Tuff from the Racer Canyon Tuff, especially where they are in fault contact. The Leach Canyon Tuff is about 25 Ma (Rowley and others, 1979; new decay constants applied). Thickness of the formation ranges from 450 feet (137 m) to about 600 feet (183 m).

Two regional ash-flow tuffs of the Condor Canyon Formation (Tcc) overlie the Leach Canyon Tuff: the lower Swett Tuff Member and upper Bauers Tuff Member. An andesitic mudflow breccia (Tccv) that thickens to the north separates the tuffs throughout much of the district. Where strongly altered, and especially where the intervening mudflow breccia is absent, the two tuffs are not distinguishable. Both ash-flow tuffs are densely welded, vitric-crystal tuffs of rhyolitic to rhyodacitic composition and contain approximately 15 percent phenocrysts of plagioclase, sanidine, biotite and minor Fe-Ti oxides. Both tuffs, particularly the Bauers Tuff, contain distinctive, light gray, flattened lenticules. Hydrothermal alteration destroyed the basal virtrophyres of these and other ash-flow tuffs in the district. The average thickness for the formation is 350 feet (107 m). K-Ar dates are about 24 Ma for the Swett Tuff Member and 23 Ma for the Bauers Tuff Member (Rowley and others, 1979; new decay constants applied).

By far the most distinctive ash-flow tuff in the district is the Harmony Hills Tuff (Th), which is the uppermost formation of the Quichapa Group. This tuff is moderately welded, dacitic, and crystal rich. Crystal content of the tuff is about 50 percent, consisting of plagioclase, biotite, hornblende, quartz, and pyroxene. Hydrothermal alteration of the formation resulted in a purplish-colored rock containing conspicuous, argillized plagioclase crystals. Thickness of the tuff ranges from 200 to 400 (60 to 120 m). K-Ar ages for the tuff range from 19.8 to 21.3 Ma.

Overlying the Harmony Hills Tuff, and tentatively included in the Quichapa Group, is a widespread andesitic mudflow breccia (Tv). The volcaniclastic unit contains cobble-sized clasts of andesitic lava and Harmony Hills Tuff with locally abundant crystal fragments derived from the underlying Harmony Hills Tuff. Thickness of the unit is approximately 100 feet (30 m). This unit occupies the same stratigraphic position as the Irontown Member of the Page Ranch Formation (Cook, 1957), but because of lithologic dissimilarities it is probably unrelated to the Page Ranch Formation.

**Racer Canyon Tuff**—The Racer Canyon Tuff (Tr) is the youngest regional ash-flow tuff in the district and marks the end of subduction-related magmatism. This is a moderately-welded, light-colored, crystal-vitric tuff containing 40 to 50 percent phenocrysts. Phenocrysts include quartz, plagioclase, sanidine, biotite, and minor Fe-Ti oxides, hornblende, and sphene. Plagioclase is ubiquitously altered within the district. Confusion with the Leach Canyon Tuff may arise in areas of strong alteration; however, the two units can be distinguished by modal analysis. Locally, a quartz-rich tuffaceous interbed (Tri) occurs near the top of the unit, presumably marking a period of reworking of the top of a lower cooling unit. A wide range of thicknesses, from 300 to 1100 feet (90 to 330 m), occurs across the district. K-Ar analyses of the tuff indicate an age of about 19 Ma (Noble and McKee, 1972; Siders, unpublished data).

**Volcaniclastic rocks of Newcastle Reservoir**—A thick volcaniclastic sequence, the volcaniclastic rocks of Newcastle Reservoir (Tnv, Shubat and Siders, 1988), overlies the Racer Canyon Tuff in the northern and southern portions of the district and and consists of interbedded volcanic conglomerate and sandstone. Its regional distribution (Siders and Shubat, 1986) shows that the volcaniclastic rocks filled an east-trending depression along the northern flank of the iron axis (figure 2). Mapping in the Silver Peak quadrangle (Shubat and Siders, 1988) revealed a great thickness of the unit lying just south of the district. The unit is absent, however, in the west-central part of the district where younger rhyolites rest directly on the Racer Canyon Tuff. A maximum thickness of 1200 feet (365 m) occurs in the northern portion of the district. This unit (formerly called the "mine series" by Siders, 1985) is the host for silver mineralized veins at the Escalante mine. Siders (1985) bracketed the age of the unit between 19 and 11.6 Ma.

**Rhyolite of Silver Peak**—The rhyolite of Silver Peak (Trs) consists of several coalescing flows and domes of rhyolite and trachyte. A textural variant of this unit, consisting of auto-brecciated flows (Trab), was also mapped. A thin, discontinuous, partially reworked air-fall tuff (Ts) locally underlies the rhyolite. Phenocrysts include quartz (6 to 10 percent), sanidine (9 percent), plagioclase (1 percent), minor biotite, and traces of Fe-Ti oxides. Phenocrysts are less than 3 mm in diameter and are set in a purplish-gray, largely devitrified matrix. Total area covered by the rhyolite is approximately 2.5 square miles (6.5 $km^2$), mostly within the Newcastle quadrangle. However, the exposed size of the rhyolite complex is limited through truncation by the Antelope Range range-front fault. The rhyolite yielded a K-Ar date of 8.4 ± 0.4 Ma.

**Dacite of Bullion Canyon**—The dacite of Bullion Canyon (Td) consists of two domes locally underlain by a volcaniclastic mudflow breccia of dacitic composition (Tdmb) and by a dacitic air-fall tuff (Tdt). The dacite domes have a purplish, devitrified matrix with coarse (7 to 12 mm) phenocrysts of quartz (12 percent), sanidine (5 percent), plagioclase (17 percent) biotite (3 percent) and Fe-Ti oxides (1 percent). Development of a diktytaxitic texture resulted in approximately 12 percent void space. The two domes are both about 3000 feet (915 m) in diameter, with concentric, steeply dipping flow-banding. Dacite domes are truncated by the western bounding fault of the Antelope Range. K-Ar analyses yielded an age of 8.5 ± 0.4 Ma, essentially identical in age to the rhyolite of Silver Peak. Field relationships, however, suggest that the dacite is slightly younger than the rhyolite.

**Quaternary Units**—Quaternary units present in the district include an older, deeply dissected fan deposit (QTaf, plate 1) and a series of Pleistocene to Holocene deposits. Younger fans were divided into two groups based on their age relative to the most recent displacement along the range-front fault of the Antelope Range. Other Quaternary deposits include pediment gravels, colluvium, and recent alluvium.

## STRUCTURE

Three distinct periods of deformation affected rocks in the Antelope Range mining district; Late Cretaceous compression, middle to late Miocene extension, and late Miocene to Quaternary basin-range style extension.

### Late Cretaceous Structures

Compressional deformation during the Late Cretaceous produced a northeast-trending anticlinal structure, locally overthrust, which extends from the Bull Valley Mountains through the Iron Springs district (Blank and Mackin, 1967). This fold-and-thrust style of deformation occurred during the Sevier orogeny (Mackin and others, 1977; Rowley and Barker, 1978). Mackin (1947) named the structure the Iron Springs Gap thrust fault in the Iron Springs district. Lewis (1958) termed the structure the Calumet fault near the Iron Mountain pluton. The thrust is interpreted to be a detachment surface between the Carmel Formation and Navajo Sandstone northwest of the Iron Mountain pluton and to ramp upward through the Iron Springs Formation along the axis of the pluton (Lewis, 1958). Results from deep wells drilled to test the hydrocarbon potential of the Moenkopi Formation confirmed the presence of thrust faults north and east of the district. Hunt Oil's Table Butte well, located just west of Table Butte, encountered the Navajo Sandstone at a depth of 9306 feet

(2838 m), beneath a sequence of Mississippian and Devonian limestones. Arco's Three Peaks well, drilled near Iron Springs, cut a repeated section of the Carmel Formation with intercalated, laccolithic quartz monzonite, the trace of the thrust being less than 2000 feet (610 m) deep.

Although not exposed, the thrust is inferred to underlie the Antelope Range district and to have minimal stratigraphic offset. Mapping in the Bullion Canyon area revealed a gentle domal structure in the Iron Springs Formation that may be related to Sevier-age deformation.

### Middle to Late Miocene Structures

Figure 4 is a fault map of the Antelope Range district showing the dominant northwest-trending structural grain. All faults shown in figure 4, except for the Antelope Range fault, belong to a generally northwest-trending, Miocene-age group of faults. The onset of this period of faulting is younger than 21 to 19 Ma, which are the ages of the Harmony Hills and Racer Canyon Tuffs. Faults of this group locally cut the dacite of Bullion Canyon and the rhyolite of Silver Peak (dated at 8.5 Ma). Reconnaissance mapping in the Newcastle quadrangle revealed that the rhyolite of Silver Peak hosts many minor faults and shows local strong hydrothermal alteration whereas the dacite of Bullion Canyon contains only sparse minor faults and is relatively fresh. The rhyolite and dacite units are both truncated by the range-front fault of the Antelope Range,

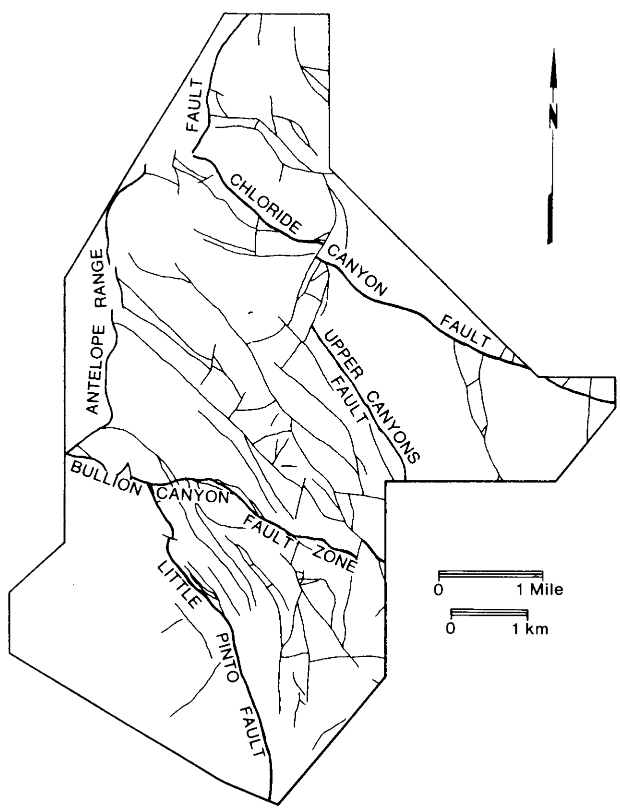


**Figure 4.** Mapped faults of the Antelope Range mining district. Named faults are described in text.

which also truncates the northwest-trending structural grain. These relationships suggest that the minimum age of the northwest-trending group of faults (and the maximum age of the range-front fault of the Antelope Range) is slightly less than 8.5 Ma.

Two dominant styles of faulting characterize this period of deformation: (1) northwest-striking (averaging N30°W) normal faults and (2) west-northwest-striking dextral to oblique-slip faults. Only two faults or fault zones in the district, the Bullion Canyon fault zone and Chloride Canyon fault, have known or suspected dextral displacement.

Named faults of the first style (northwest-striking normal faults) are the Little Pinto and Upper Canyons faults (figure 4). Minimum stratigraphic separations for these faults are 2000 feet (610 m) and 2800 feet (850 m), respectively. Both faults dip moderately to the southwest; dips of about 50° were measured from exposures of the Little Pinto fault. Drill hole data indicate a moderate dip for some other faults of this group. The dominance of slickensides with rakes of approximately 90° measured on exposures of the Little Pinto fault and a normal sense of stratigraphic separation suggest that these are dominantly normal faults. Local stratal rotations of as much as 60° in the volcaniclastic rocks of Newcastle Reservoir suggest a listric-normal geometry for at least some of these faults.

West-northwest-striking, dextral to oblique-slip faults were also produced during this period of extension. A dextral component of displacement of 3200 feet (976 m) was calculated for the Chloride Canyon fault, based on a piercing point reconstruction (Shubat and Siders, 1988). Evidence for a dextral component of displacement along the Bullion Canyon fault zone is the presence of well-developed horizontal slickensides on several exposures with dominantly dextral slip indicators. Drill hole data show that the Bullion Canyon fault zone dips moderately (48° to 60°) to the southwest. Normal stratigraphic separation across the Bullion Canyon fault zone is as much as 1950 feet (600 m).

### Late Miocene to Quaternary Structure

Late Miocene to Quaternary deformation in the Antelope Range district produced the Antelope Range fault (figure 4). This fault, with a surface expression typical of basin-range style faults, forms the boundary between the Antelope Range and the Escalante Valley. Quaternary fault scarps delineate the fault and extend northeastward from the western margin of the Antelope Range district (figure 4) to the center of the Antelope Peak quadrangle and southwestward to the south-central portion of the Newcastle quadrangle. Near Newcastle the fault exerts a control on the Newcastle geothermal system (Clement, 1980). The Antelope Range fault appears to truncate all structures within the range.

A prominent gravity low was discovered immediately west of the Antelope Range in a gravity survey of the Escalante Valley (Pe and Cook, 1980). This gravity low may represent a thickness of as much as 10,000 feet (3 km) of alluvium. Pe and Cook (1980) named this feature the Newcastle graben. Displacement along the Antelope Range fault presumably formed the eastern margin of the Newcastle graben and suggests that vertical separation across the fault may be in excess of 10,000 feet (3 km). Rapid uplift of the Antelope Range locally caused oversteepening of the range-front, resulting in a gravity-slide block in the Bullion Canyon area.

## MINERALIZATION

Known mineral occurrences in the Antelope Range district consist of base and precious metals-bearing veins, similar to many epithermal systems throughout the Great Basin. While other forms of mineralization may exist in the district (see last section), this discussion will focus on vein deposits. Commodities present in potentially economic concentrations include silver, gold, copper, lead, and zinc. The Antelope Range district is historically known as a silver district.

### FORM AND DISTRIBUTION

Veins in the Antelope Range district occur as fillings within structures. Veins typically show textures of open-space filling such as banding, cockscomb texture, and encrustation. Individual veins range in strike length from less than 100 feet (30 m) to as much as 4500 feet (1370 m). Longer veins tend to occur along major structures and smaller veins along fractures. Pinch and swell along veins is common, producing highly variable vein widths. The maximum vein width observed is 45 feet (14 m). In many places veins "horsetail" along strike, changing from a discrete vein to a series of closely spaced veinlets (stockwork zone). Veins also pass laterally (along strike) and vertically into breccia fillings. In general, vein material appears to have filled the available void space.

Plate 2 shows the locations of veins mapped in the district. A strong correspondence exists between veins and structures. The dominant vein trend mimics the dominant fault trend, with an average strike of approximately N30°W. The pattern of vein distribution also shows a clustering tendency. These areas of high vein density (vein systems) are identified by name in plate 2. One vein system, the Little Pinto, consists of a single chalcedonic vein along the Little Pinto fault and is traceable over a strike length of 7000 feet (2130 m). The Bone Hollow vein system contains about 40 individually mapped veins, primarily controlled by two faults, and extends over a strike length of approximately 10,000 feet (3050 m). Remaining vein systems have lengths ranging from 2000 to 5000 feet (610 to 1520 m) and widths of 700 to 1200 feet (210 to 370 m). A large number of veins occur throughout the Bullion Canyon area that do not show this clustering tendency. The "eastern vein area" consists of scattered veins located in the eastern portion of the district (plate 2).

Mineralized veins show a wide variation in the content of ore minerals. Because hand-sample identification of precious metals-bearing minerals is tenuous, a geochemical approach to the identification of mineralized areas was employed (see geochemistry section). A few generalizations apply to the visual appearance of mineralized veins. Base metals-enriched veins contain sparse original sulfides (galena, pyrite, and chalcopyrite), a quartz, calcite, and barite gangue assemblage, and supergene cerussite, malachite, chrysocolla, and brochantite. Silver-rich veins are quartz dominated, vuggy, show some base metals enrichment, and contain abundant barite and rose-colored to amethyst quartz. Gold-enriched systems tend to be more chalcedony-rich and may contain fine-grained, disseminated pyrite.

### ORE AND GANGUE MINERALOGY

Identification of ore minerals employed a combination of hand sample, ore microscopy, x-ray diffraction analysis, and staining techniques. Ore minerals are typically fine grained, although supergene alteration destroyed most of the primary ore minerals originally present. Primary (hypogene) sulfides present in the veins include galena, chalcopyrite, and sphalerite. Silver is present in several hypogene sulfosalt minerals, namely pearceite ($Ag_{16}As_2S_{11}$+Cu), tennantite ($(Cu, Fe)_{12}As_4S_{13}$+Zn, Ag), stromeyerite (CuAgS), and proustite ($Ag_3AsS_3$). Supergene ore minerals identified include tenorite (CuO), cuprite ($Cu_2O$), covellite (CuS), digenite ($Cu_9S_5$), malachite ($Cu_2CO_3(OH)_2$), brochantite ($Cu_4(OH)_6SO_4$), chrysocolla ($Cu_2H_2(Si_2O_5)(OH_4)$), cerussite ($PbCO_3$) (confirmed by x-ray diffraction), and smithsonite ($ZnCO_3$).

Primary gangue minerals are quartz, calcite, chalcedony, barite, pyrite, and psilomelane. Vein quartz crystals are clear with milky zones and are locally amethystine. Calcite ranges in color from white to brown to black. X-ray diffraction analysis of dark-colored vein carbonate shows the presence of manganoan calcite and a complex manganese mineral similar to psilomelane or manganite. Barite occurs in blades, as much as an inch long, intergrown with quartz and calcite. Although generally present in quantities less than 1 percent, one vein sample from the district contained 47.1 percent barite. Secondary gangue minerals identified include hematite, goethite, and braunite ($3Mn_2O_3.MnSiO_3$).

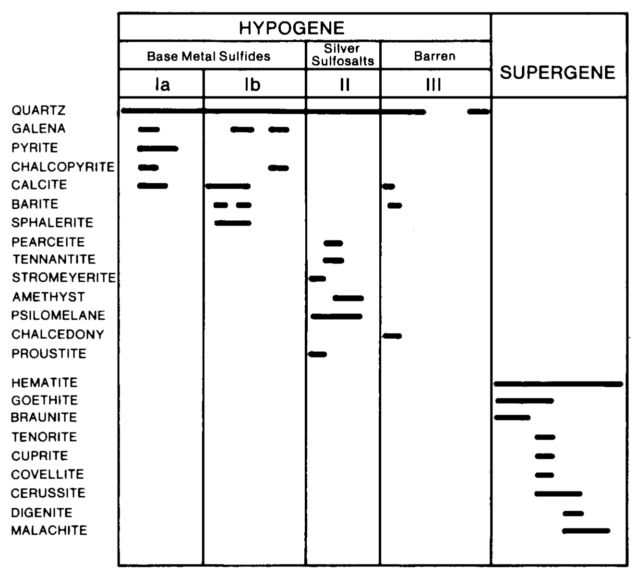


**Figure 5.** Paragenetic history of ore and gangue mineral deposition for veins in the Bullion Canyon area.

## PARAGENESIS

Examination of polished sections of sulfide-bearing vein material from the Bullion Canyon area resulted in an opaque mineral paragenesis (figure 5). Thin sections and slabbed hand samples provided information on gangue mineral paragenesis. Figure 5 summarizes the results of this study. The entire sequence is not present in every vein.

The appearance of two different suites of sulfide minerals defines two hypogene mineralization stages. Stage I mineralization produced base metals sulfides, partially replaced by silver sulfosalts in stage II. During stage I mineralization, galena, chalcopyrite, and sphalerite coprecipitated with quartz, calcite, local barite, and pyrite. Thin sections and hand samples show these early (stage I) base metals sulfides associated with milky bands in cockscomb quartz gangue. Milky bands are inclusion-rich and contain explosion textures. Stage II silver minerals precipitated in association with quartz, amethyst, and psilomelane. Calcite is absent from this stage. Silver minerals that form solid solution series were assumed to be the arsenic-rich variety because of the abundance of arsenic relative to antimony (see geochemistry section). By the end of stage II, sulfide deposition ceased and stage III gangue minerals (including quartz, calcite, barite, and chalcedony) precipitated. The stage III event formed fine-grained quartz veinlets that cut chalcedony veinlets. During the supergene stage, oxides and carbonates largely replaced original sulfides.

## FLUID INCLUSIONS

Milky zones in cockscomb vein quartz from the Bullion Canyon area contain explosion textures and abundant fluid inclusions. Two types of fluid inclusion occur, type I and type II inclusions of Nash (1976). Type I inclusions (liquid dominated, moderate salinity) are the most abundant with lesser type II (vapor dominated, moderate salinity) inclusions present. Type II inclusions occur in spatial association with explosion textures in quartz crystals and in association with barite and calcite. Measurement of fluid inclusion homogenization temperatures ($T_h$) using both primary and pseudosecondary inclusions from boiling (indicated by explosion textures), pre-boiling, and post-boiling zones (figure 6), followed procedures outlined by Roedder (1984).

Results show a wide variation in $T_h$ measured from fluid inclusions in the same zone and indicates trapping with variable liquid to vapor ratios. This is characteristic of inclusions formed during boiling (Kamilli and Ohmoto, 1977). The lowest homogenization temperature measured from boiling stage inclusions yields the true temperature of trapping without requiring a pressure correction. This gives a boiling range of 198° to 205°C for veins in the Bullion Canyon area. Using temperature-versus-depth charts from Hass (1971), the $T_h$ of inclusions from boiling zones, and an assumed salinity of 10 weight/percent NaCl, the estimated depth to the boiling level at the time of mineralization is 460 feet (140 m). This figure, however, is less than the present vertical exposure of the Bone Hollow vein system, possibly the result of the $CO_2$ content of the system. As discussed by Hedenquist and Henley (1985), knowledge of the $CO_2$ content of hydrothermal solutions can significantly increase the depth of formation estimates for epithermal deposits. Thus the estimate of 460 feet (140 m) mentioned above is a minimum depth of formation.

## AGE RELATIONS

No direct measurements of the age of mineralization were possible because of the paucity of potassic alteration phases suitable for dating. Field evidence, however, places constraints on age. It is assumed throughout this discussion that mineralization and hydrothermal alteration were both produced by the same hydrothermal system and that mineralization occurred as distinct events within the longer history of the hydrothermal system.

Field evidence shows that veins occur as open-space fillings within structures. This implies that formation of the structures pre-dated vein filling. Arguments presented above show that northwest-striking faults probably formed between 21 and 8 Ma. Some veins show evidence of repeated brecciation and filling (as in the Little Pinto vein) and others show late brecciation with no filling. Many veins, however, do not show evidence of late brecciation. Critical age relationships exist where the Bone Hollow vein system intersects the Bullion Canyon fault zone (plate 2). The Bone Hollow vein system crosscuts the Bullion Canyon fault zone without offset. In addition, stratigraphic separation across primary faults of the Bone Hollow system appears to terminate to the north against the Bullion Canyon fault zone (plate 1). These relationships are interpreted as follows: displacement along faults of the Bone Hollow system and the Bullion Canyon fault zone occurred contemporaneously, and vein formation occurred after all displacement had ceased along the Bullion Canyon fault zone. Two observations provide additional constraints on the age of hydrothermal alteration and mineralization. First, the 8.5 Ma dacite of Bullion Canyon is only locally altered, whereas the rhyolite of Silver Peak is more pervasively altered, suggesting that much of the alteration occurred between the eruption of rhyolite and dacite flows. Second, the Antelope Range fault appears to truncate mineralized structures and to cut rhyolite and dacite flows, and thus is presumably younger than the

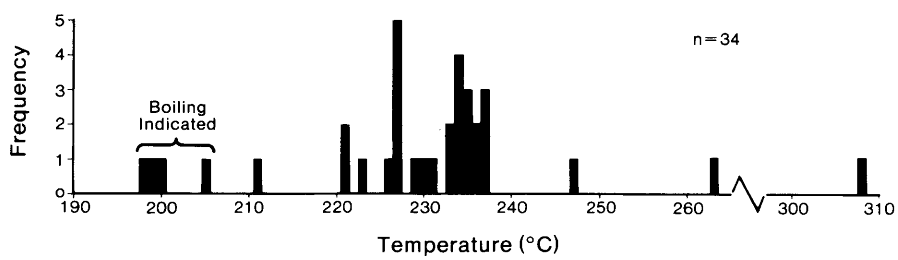


**Figure 6.** Fluid inclusion homogenization temperatures ($T_h$) from the Bullion Canyon area. Height of bar represents the number of inclusions measured (frequency) of that temperature, n is the total number of inclusions measured.

mineralizing event. In summary, these observations suggest that alteration and mineralization were approximately contemporaneous with 8.5 to 8.4 Ma rhyolite and dacite volcanism.

## HYDROTHERMAL ALTERATION

Plate 2 shows mapped hydrothermal alteration zones in the Antelope Range district. Alteration zones, defined in such a way as to be distinguishable in the field, consist of mineral assemblages confirmed by petrographic examination and x-ray diffraction analysis. Two genetic types of alteration occur in the district: (1) structurally controlled alteration, and (2) pervasive alteration. Structurally controlled alteration formed as hydrothermal solutions passed through open faults and fractures, penetrating into and altering the wall rock. Porosities and permeabilities of the different lithologies, however, controlled pervasive alteration.

Many epithermal vein districts in the Great Basin show wide halos of propylitic alteration that extend as far as several miles beyond mineralized veins. However, no clearly defined propylitic halo is present in the Antelope Range district. A more subtle but equivalent form of alteration (not shown in plate 2) consists of the destruction of basal vitrophyres of ash-flow tuffs. Outside of the district, in the eastern Silver Peak quadrangle, these basal vitrophyres are ubiquitously preserved. This distal effect of alteration extends as far as 15,000 feet (4570 m) from the center of the district. Other effects of this subtle alteration include partial alteration of plagioclase to montmorillonite clays and the presence of sparse calcite veinlets. However, in hand sample, these effects are not distinguishable from weathering products.

### STRUCTURALLY CONTROLLED ALTERATION

Structurally controlled alteration, consisting of seven separate zones, encompasses all vein systems in the district, including small areas of propylitic and argillic alteration localized along faults in areas east and north of the Little Pinto vein (plate 2). Evidence of structural control, based on field observations, includes (1) an increase in intensity of alteration adjacent to veins, (2) increase in the density and size of veinlets in stockwork zones in and adjacent to faults, and (3) a general spatial correspondence between alteration zones and faults.

#### Stockwork and Structurally Controlled Silicification

This alteration zone encloses all mineralized vein systems in the district (plate 2) and consists of stockwork veinlets of quartz, calcite, and lesser chalcedony with intervening host rock showing both silicification and argillization. Volcanic units show widespread silicification of matrix material and argillization of plagioclase and pumice clasts. Plagioclase is dominantly altered to kaolinite, with lesser amounts of halloysite, and minor montmorillonite (all clays confirmed by x-ray diffraction). Calcite, chlorite, and quartz are locally present in relict plagioclase phenocrysts. Groundmass areas of porous tuffs and pumice clasts are altered to a fine-grained mixture of quartz and kaolinite. It is possible that this alteration resulted from the overprinting of silicification on previously argillized rock.

The dominant characteristic of this zone in sedimentary rocks (in the Bullion Canyon area) is the presence of silica stockwork veining. Other alteration effects in sedimentary units are silicification and bleaching of vein walls. Silicification rarely extends more than 2 inches (5 cm) and bleaching (argillization) may extend as far as several feet (1 m) from vein walls. Alteration products in bleached zones consist of kaolinite, lesser halloysite, and minor montmorillonite.

Another alteration type mapped in the district, weak stockwork and structurally controlled silicification, is similar to the zone described here. It was subjectively identified as a less intense form of the above alteration, which fringes the main area of veining and stockwork development (plate 2).

#### Potassium-Bearing Assemblages

Both phyllic and potassic alteration occur in the Antelope Range mining district. Potassic alteration consists of the assemblage adularia + quartz and occurs in highly silicified clasts lying within veins. Feldspar staining showed two occurrences of fine-grained adularia within the EBC vein system (plate 2). Phyllic alteration consists of the assemblage sericite + pyrite + quartz. Pyrite occurs as microscopic grains giving the rock a dark gray color. Sericite is present in minor amounts, its presence verified by petrographic and x-ray diffraction analysis. In hand sample, this alteration appears as a densely silicified, dark gray rock. Several small areas of this type of alteration occur where the Bullion Canyon fault zone intersects the Bone Hollow vein system (plate 2).

### PERVASIVE ALTERATION

Pervasive alteration, alteration controlled by lithology rather than by structure, occurs in the southwest corner of the district, lying southwest of the Little Pinto vein (plate 2). Three alteration assemblages are present: argillic alteration, extreme silicification, and kaolinitic alteration. Argillic alteration is the dominant assemblage of pervasive alteration.

Original porosity probably controlled the distribution of argillic alteration in the Racer Canyon Tuff and the rhyolite of Silver Peak. Mineralogy of the argillic assemblage consists of kaolinite, chalcedonic quartz, and calcite, with minor halloysite and montmorillonite (identified by x-ray diffraction). Plagioclase alteration products are kaolinite and minor calcite. Sanidine, quartz, and biotite are mostly fresh. The groundmass of argillized Racer Canyon Tuff consists of a fine-grained mixture of kaolinite and chalcedonic quartz.

Extreme silicification is restricted to a reworked interbed within the Racer Canyon Tuff (Tri, plate 1) and areas immediately adjacent to the Little Pinto vein. The alteration zone constitutes a complete replacement of the host by silica (dominantly chalcedonic), except for remnant quartz phenocrysts. This alteration, best developed just west of the Little Pinto fault, apparently formed as silica-bearing solutions rose along the Little Pinto fault (producing the chalcedonic Little Pinto vein) and encountered the highly porous and permeable interbed.

Kaolinitic alteration consists of a fine-grained mixture of kaolinite, silica, and calcite (secondary?), representing the effects of acid leaching. Kaolinitic alteration occurs, as shown on plate 2, in three small areas: (1) beneath the isolated patch of densely silicified Racer Canyon interbed described above, (2) at the core of a hematitic zone shown in plate 2, and (3) in the extreme southwestern corner of the district. The product of kaolinitic alteration is a white, porous rock with sparse stringers of opaline silica. The total destruction of primary textures, dominance of kaolinite, and association with intense hematitic alteration suggest that the kaolinitic alteration described here could be transitional to advanced argillic alteration. However, the presence of calcite (possibly secondary), the absence of alunite, and the relative sparseness of opaline silica argue against classification as advanced argillic alteration.

## GEOCHEMISTRY

To evaluate the mineral potential of the Antelope Range district, a database consisting of 1957 trace metal analyses and supporting descriptive and mineralogical data was compiled. Three sources of information for this database are: (1) data donated by the Tenneco Minerals Company, (2) data collected by one of the authors (W. McIntosh) with analytical support donated by the Homestake Mining Company, and (3) data collected by the Utah Geological and Mineral Survey. Figure 7 shows the distribution of geochemical samples, the locations of 13 diamond drill holes for which geochemical data were available, and the outlines of major vein systems.

Sample types represented in the data base include rock-chip, grab, dump, trench, and drill-core samples. Approximately two-thirds of the database consists of rock-chip samples collected from surface exposures. The remaining third is mostly drill-hole data. Descriptions of samples collected by the authors accompany analytical data for Au, Ag, Cu, Pb, Zn, and As.*

Interpretation of the data was facilitated by the creation of several subsets. Data were spatially separated in order to preserve the geochemical uniqueness of each major vein system and were also separated by source to minimize laboratory bias. Where appropriate, data from each of the systems was further divided into sets based on the presence or absence of veins and vein mineralogy.

Tables 1 through 5 summarize univariate statistics for each area. Selection of anomalous thresholds involved comparing (1) the mean plus two standard deviations, (2) the 90th percentile, and (3) prominent gaps in histograms. Removal of outliers (highly mineralized samples) allowed selection of meaningful anomalous thresholds. In the following discussion, thresholds of significance for the correlation coefficients (calculated using the methods of Snedecor and Cochran, 1980, at the 95 percent confidence level) follow the coefficient in parentheses.

### BLAIR DATA SET

Geochemical data for the Blair vein system (figures 7 and 8) consist of fire assays for Au and Ag (table 1). Most samples are rock-chip samples from surface exposures of quartz + calcite veins. Vein locations are shown in plate 2. Base metal analyses for 18 samples (table 1) show a strong mutual correlation between Cu, Pb, and Zn, with coefficients ranging from 0.78 to 0.92 (threshold = 0.47), and a weak (but not significant) correwith Ag (coefficients ranging from 0.21 to 0.26, threshold = 0.47).

Precious metals data show that the Blair vein system is strongly enriched in Ag. In comparison to the remainder of the district, vein samples from the Blair area have a much higher average silver concentration (21.6 ppm as opposed to 5 ppm) and anomalous threshold for silver (60 ppm as compared to 15 ppm). Au values for vein samples, however, are uniformly low; of 194 samples analyzed, only five were above the lower detection limit for Au (.171 ppm). Three of these five analyses are from surface samples (figure 8). The remaining two gold values are from quartz vein samples from drill hole 12 (figure 8). A correlation coefficient of -0.01 (threshold = 0.14) for Au and Ag indicates that no consistent relationship exists between these elements.

Figure 8 shows the locations of anomalous Ag values in the Blair area. Ag values show strong enrichment in two quartz veins, both of which lie along the same linear trend and may occupy the same structure (the 'west Blair vein' DDH 12, figure 8). Drilling results near the west Blair vein proved disappointing in that only a few, thin veins were encountered yielding a maximum silver value of only 24 ppm. Because the vein dips to the southwest at the surface and because drill hole 12 projects to a point directly beneath the surface trace of the vein (figure 8), it is possible that the hole did not penetrate the west Blair vein. Drill hole 13 also encountered a few veins, the largest of which has an apparent thickness of 12 feet, is calcite-rich, and yields a maximum Ag value of 51 ppm.

### BULLION CANYON DATA SET

A total of 250 samples (199 from veins) constitute the Bullion Canyon data set. Mineralogical and descriptive data for each sample accompany analytical data. Most samples are rock-chip samples from surface exposures. Sixteen samples are grab samples from dumps.

Univariate statistics for Bullion Canyon data (table 2) show that Au, Ag, Cu, Pb, and Zn are markedly enriched in vein samples. The element As, however, is rarely enriched in veins. Interpretation of data employed the use of two levels of anomalous thresholds. First, threshold levels above the 95th percentile defined highly anomalous values (obviously mineralized). These outliers were removed and univariate statistics recalculated for the remaining data. Lower level anomalous thresholds were then selected and used to create maps of anomalous values for Au, Ag, Cu, Pb, Zn, and As (figures 9 through 14).

*Samples collected by the UGMS were analyzed for a 20 element suite by neutron activiation analysis (Bondar-Clegg Inc., Lakewood, Colorado). This suite consists of: Au, Ag, Cu, Pb, Zn, As, Sb, Ba, W, Mo, Na, Cr, Fe, Co, Ni, Se, Cd, La, Hf, Ta, Ir, Th, and U. Analyses of Cu, Pb, and Zn were obtained by atomic absorption. Lower detection limits are: Au, 5 ppb; Ag, 5 ppm; Cu, 1 ppm; Pb, 1 ppm; Zn, 1 ppm; As, 0.5 ppm; Sb, 0.2 ppm. Samples collected by W. McIntosh were analayzed for Au, Ag, Cu, Pb, Zn, and As, and some for Sb and Hg. Analytical methods were fire assay for Au and Ag, and atomic absorption for the remaining elements. Lower limits of detection are: Au, 1 ppb; Ag, 0.01 ppm; As, 1 ppm; Cu, 1 ppm; Pb, 1 ppm; Zn, 5 ppm; Sb, 1 ppm; Hg, 10 ppb. Data from Tenneco Minerals Company consist largely of fire assays for Au and Ag, and some analyses for Cu, Pb, Zn, Mo, As, Sb, and Hg.

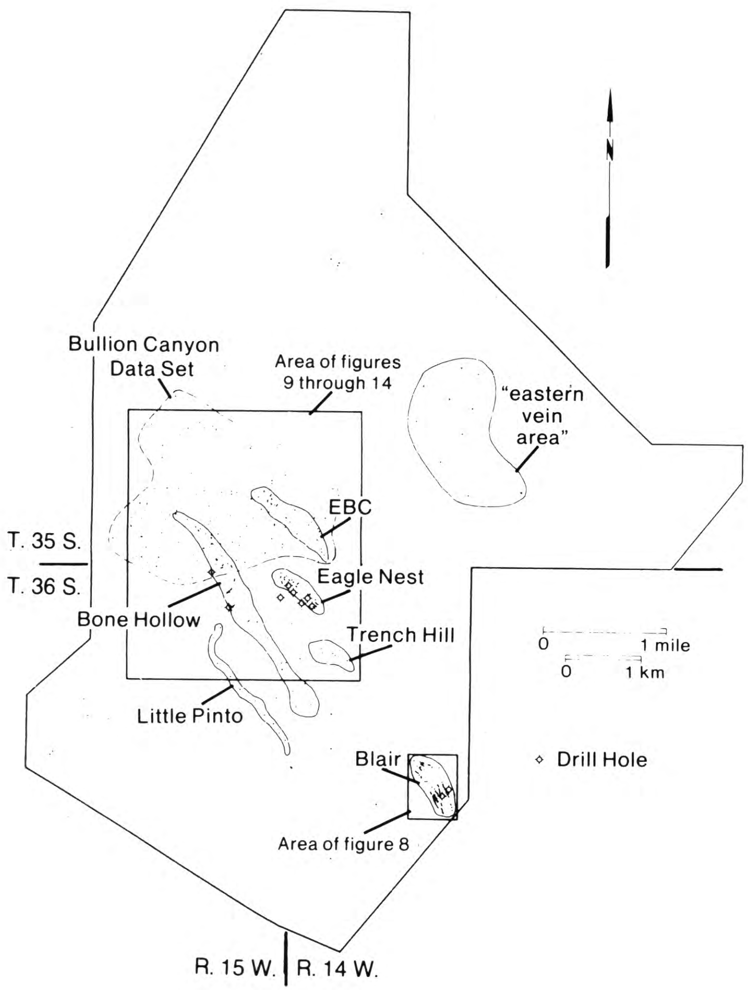


**Figure 7.** Distribution of geochemical sampling sites (small dots) for the Antelope Range mining district. Also shown are drill-hole locations and the outlines of named vein systems. Dashed line encloses sampling sites for the Bullion Canyon data set.

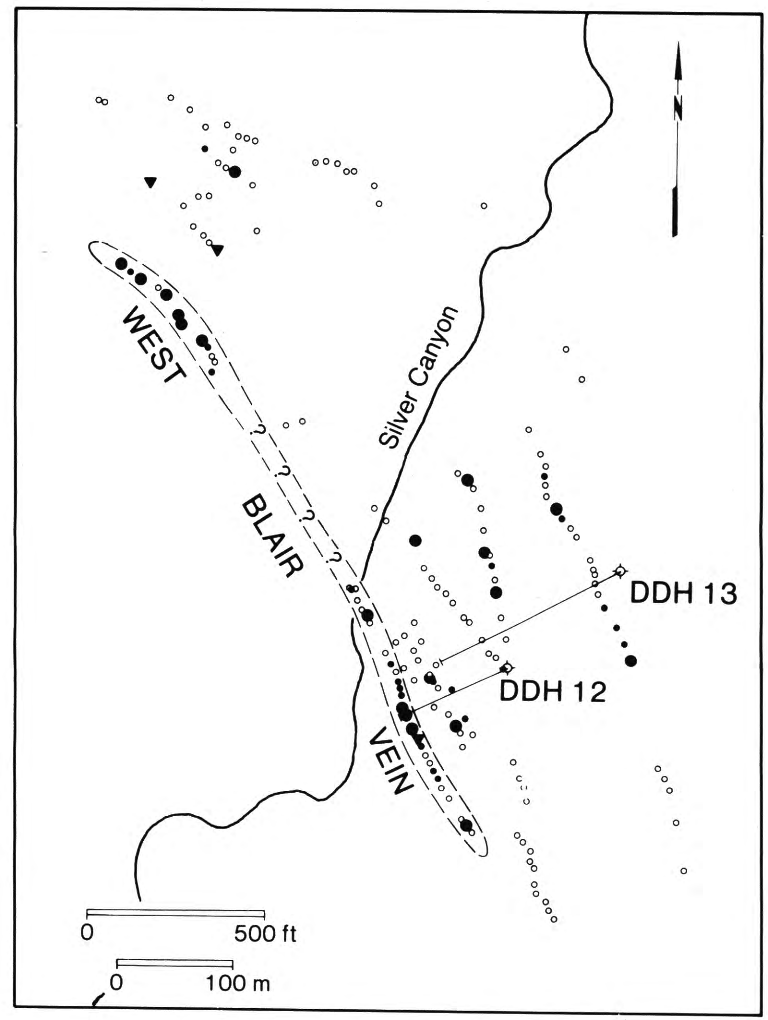


**Figure 8.** Geochemical anomaly map for the Blair vein system. Large solid dots represent silver values greater than 60 ppm (anomalous). Small solid dots represent silver values between 25 and 60 ppm. Solid triangles represent gold values greater than 0.34 ppm. Sample sites without anomalous values shown as open circles. Also shown are collar locations and horizontal projections of diamond drill holes.

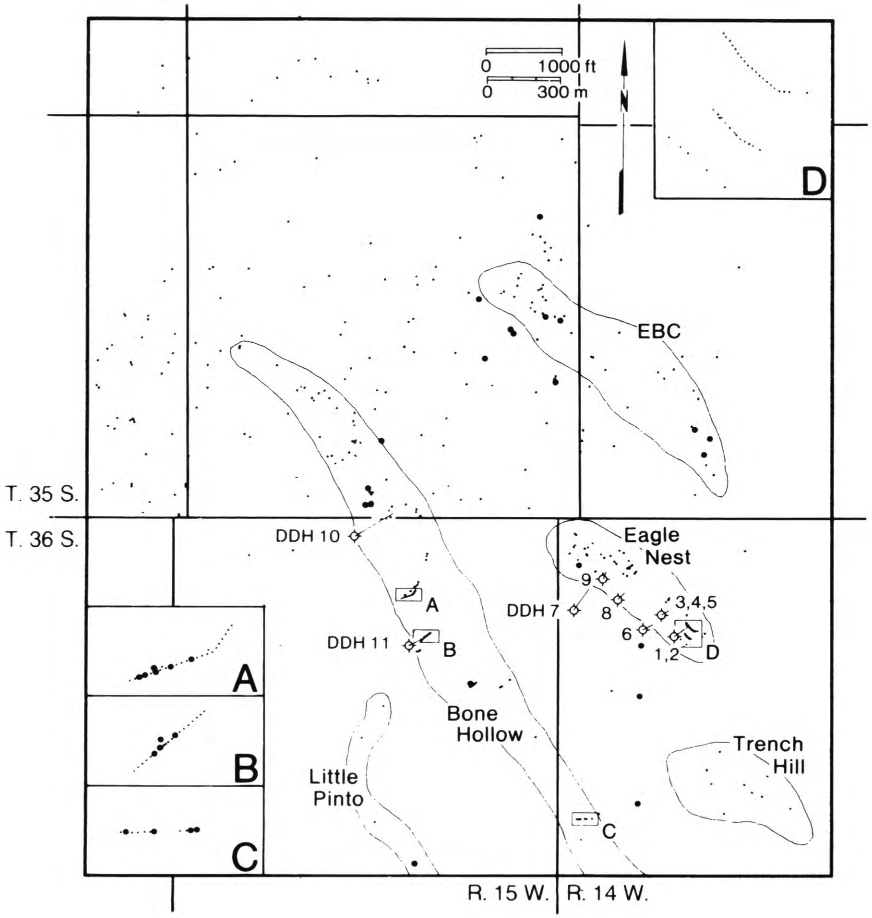


**Figure 9.** Gold anomaly map for Bullion Canyon and adjacent area. Large dots represent gold values greater than 0.48 ppm. Small dots are the remaining sample sites. Also shown are the outlines of named vein systems and diamond drill-hole locations from figure 7.

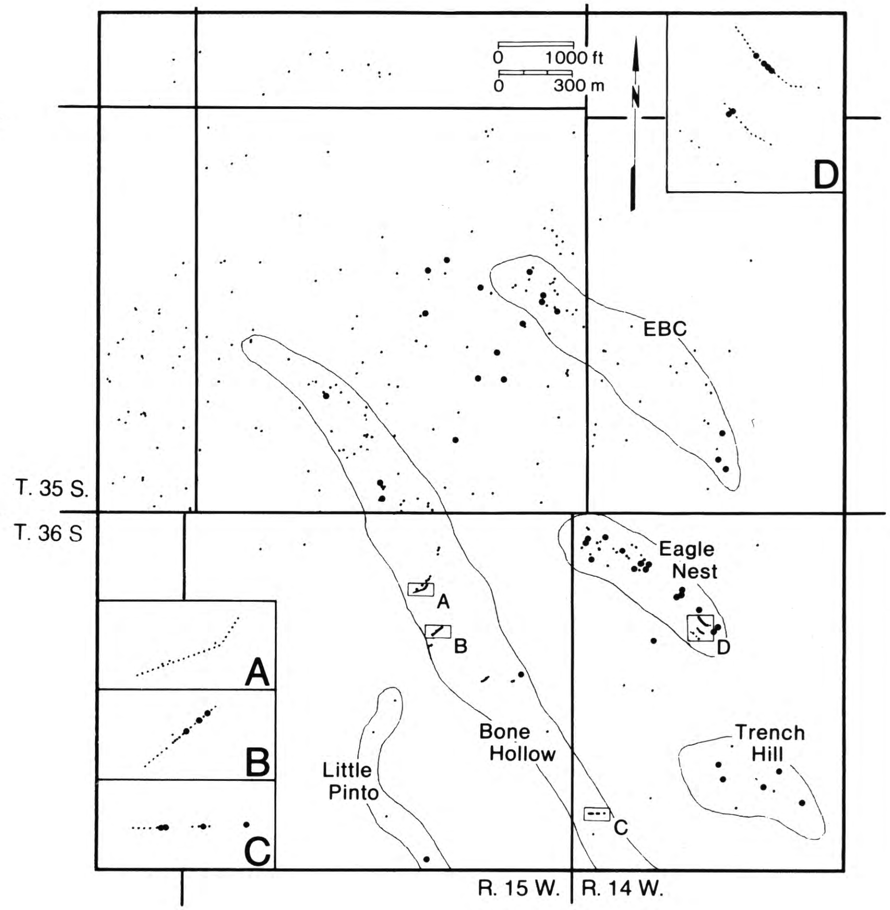


**Figure 10.** Silver anomaly map for Bullion Canyon and adjacent area. Large dots represent silver values greater than 15 ppm. Small dots are the remaining sample sites. Named vein systems are outlined.

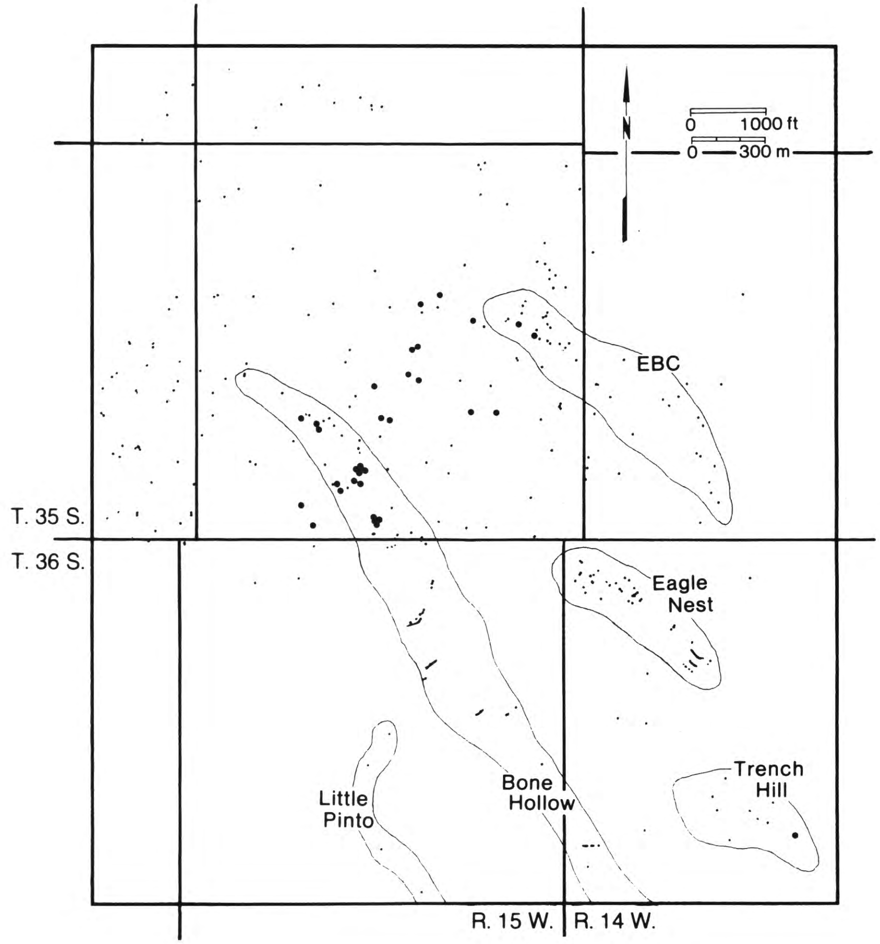


**Figure 11.** Copper anomaly map for Bullion Canyon and adjacent area. Large dots represent copper values greater than 800 ppm. Small dots are the remaining sample sites. Named vein systems are outlined.

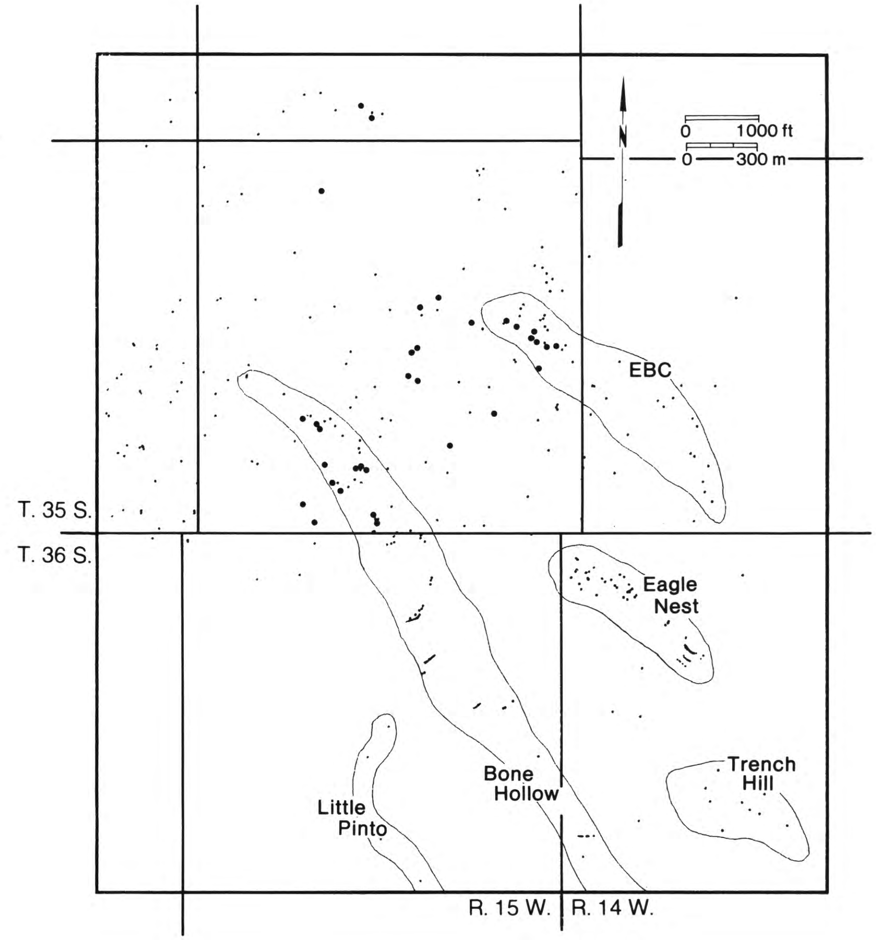


**Figure 12.** Lead anomaly map for Bullion Canyon and adjacent area. Large dots represent lead values greater than 3400 ppm. Small dots are the remaining sample sites. Named vein systems are outlined.

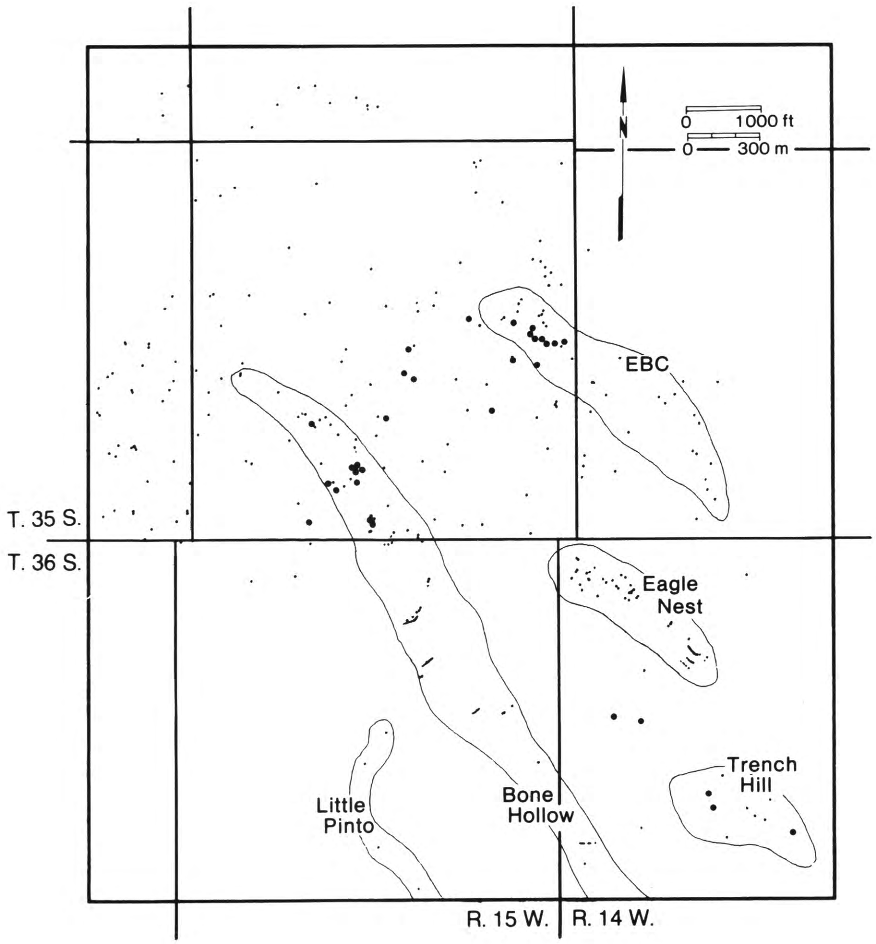


**Figure 13.** Zinc anomaly map for Bullion Canyon and adjacent area. Large dots represent zinc values greater than 3100 ppm. Small dots are the remaining sample sites. Named vein systems are outlined.

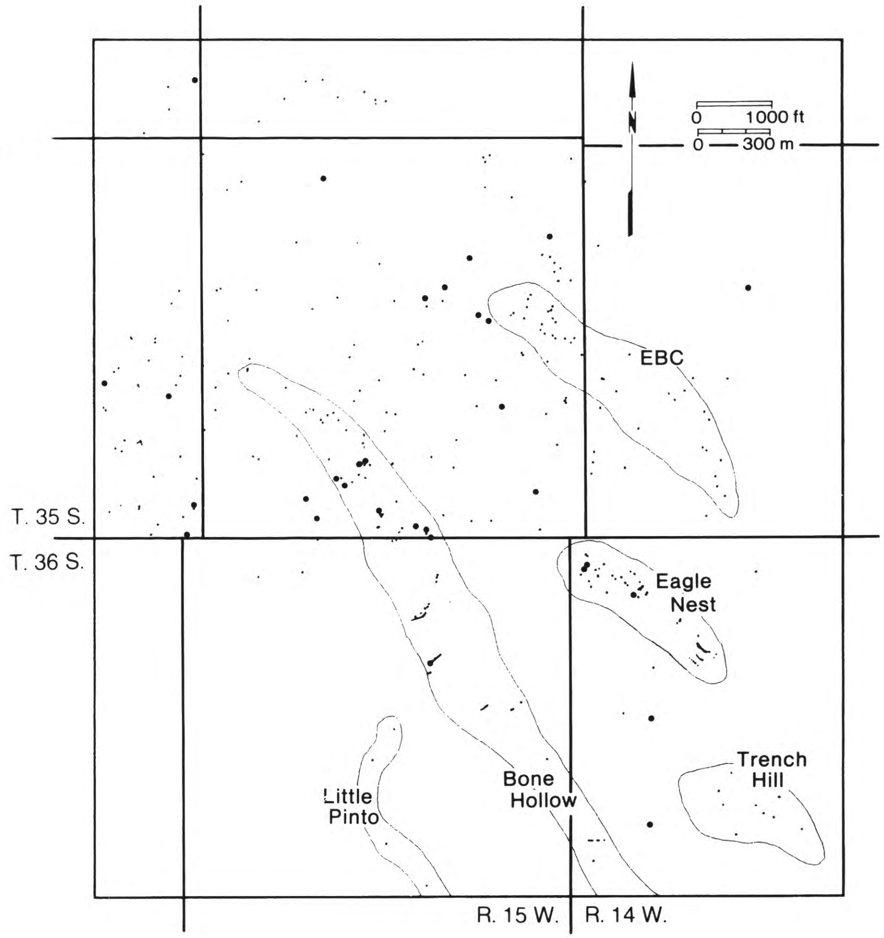


**Figure 14.** Arsenic anomaly map for Bullion Canyon and adjacent area. Large dots represent arsenic values greater than 225 ppm. Small dots are the remaining sample sites. Named vein systems are outlined.

Table 1. Univariate statistics for the Blair data set, Antelope Range mining district. All values are in parts per million

| Element | n* | Mean | Maximum | Minimum** | Standard Deviation | 90th Percentile | Anomalous Threshold |
|---|---|---|---|---|---|---|---|
| Au | 195 | .053 | 6.17 | .001 | .46 | — | See text |
| Ag | 194 | 21.9 | 276.3 | .1 | 36.5 | 64.8 | 60.0 |
| Cu | 18 | 560 | 6000 | 10 | — | — | — |
| Pb | 18 | 255 | 1750 | 5 | — | — | — |
| Zn | 18 | 437 | 1800 | 55 | — | — | — |

*n = Number of examples

** = Minimum value or lower limit of detection

Table 2. Univariate statistics for the Bullion Canyon data set, Antelope Range mining district. All values in parts per million.

| Subset | Element | n* | Mean | Maximum | Minimum** | Standard Deviation | 90th Percentile | Threshold for highly anomalous samples |
|---|---|---|---|---|---|---|---|---|
| Vein Samples | Au | 199 | .23 | 7.19 | .001 | .85 | .3 | 1.6 |
| | Ag | 199 | 5.7 | 88.4 | .1 | 11.1 | 16 | 45.0 |
| | Cu | 199 | 368 | 6700 | 1 | 854 | 1050 | 2000 |
| | Pb | 199 | 1491 | 27,000 | 1 | 3599 | 4830 | 8000 |
| | Zn | 199 | 1321 | 26,000 | 5 | 3086 | 3871 | 8000 |
| | As | 199 | 112 | 3100 | 1 | 269 | 208 | 510 |
| Non-Vein Samples | Au | 51 | .06 | .82 | .001 | .13 | .16 | |
| | Ag | 51 | 1.9 | 37.3 | .1 | 5.3 | 3.1 | |
| | Cu | 49 | 95 | 2600 | 1 | 380 | 150 | |
| | Pb | 51 | 119 | 1800 | 1 | 227 | 201 | |
| | Zn | 51 | 214 | 3800 | 1 | 359 | 254 | |
| | As | 51 | 69 | 380 | 1 | 91 | 228 | |
| | | | | | | | | Anomalous thresholds, outliers removed |
| Vein Samples with Outliers Removed | Au | 195 | .12 | 1.50 | .001 | .24 | .32 | .48 |
| | Ag | 195 | 4.7 | 40.1 | .1 | 7.1 | 14.8 | 15.0 |
| | Cu | 188 | 194 | 1900 | 1 | 356 | 647 | 800 |
| | Pb | 189 | 802 | 7800 | 1 | 1545 | 2627 | 3400 |
| | Zn | 191 | 825 | 7700 | 5 | 1401 | 3083 | 3100 |
| | As | 195 | 81 | 500 | 1 | 92 | 182 | 225 |

*n = Number of samples

** = Minimum values or lower limit of detection

## EAGLE NEST DATA SET

Data from the Eagle Nest area (figure 7) consist of 401 core samples and 67 surface samples. Of the surface samples, 39 are from three parallel trenches at the south end of the vein system (inset D, figures 9 and 10). Data include analyses for Au and Ag and limited analyses for base metals, arsenic, antimony, and mercury (table 3).

Anomalous thresholds were not calculated for these data for two reasons. First, the analytical method employed for Au has a lower detection limit that is too high for reliable identification of anomalous threshold values. Second, an insufficient number of analyses for base metals and arsenic exist for statistical validity. Because of these restrictions, anomalous thresholds for the Bullion Canyon data set (table 2) were applied to the Eagle Nest data. Surface samples show anomalous concentrations of Ag only (figure 10). The absence of base metals anomalies may be a function of the limited data.

Geochemical data from nine core holes drilled in the Eagle Nest area (figure 7) show anomalous concentrations of Au, Ag, Pb, Zn, and As (table 3). Gold values are generally low with only a few above the anomalous threshold. Many Pb, Zn, and Ag anomalies are present, with veins markedly enriched in these elements. Most drill holes penetrate the Bullion Canyon fault zone. In this area, the fault zone dips 48° to 65° to the south-southwest, is approximately 250 feet (76 m) wide, and contains many quartz and calcite veins separated by mylonitized and brecciated host rock. Figure 15 is a geochemical profile across the fault zone derived from data from hole 5. Quartz veins dominate in the upper portion of the fault zone and are generally enriched in base and precious metals. Calcite veins dominate in the lower part of the fault zone. Of interest is the presence of weak, but persistent, Au enrichment just beneath the lithologic contact between the Isom and Claron Formations.

## BONE HOLLOW DATA SET

Geochemical data from the Bone Hollow area, divided into drill-hole and surface sets (table 4), consist of analyses of samples from four trenches across the vein system (shown in insets A, B, and C, figures 9 and 10) and two drill holes. Data include analyses for gold and silver, and some analyses for base metals, arsenic, antimony, and mercury. Anomalous thresholds derived for the Bullion Canyon area were applied to this data set for the same reasons given for the Eagle Nest area.

Surface data show an enrichment in both Au and Ag (figures 9 and 10). A unique feature of this area compared to other vein systems is the relative enrichment in Au; this area contains the highest Au value (over 7.5 ppm), the highest Au:Ag ratios, and the greatest density of gold anomalies (figure 9). Drill hole data are not as encouraging as surface data (table 4), and only two samples (quartz veins) from hole 11 contain anomalous concentrations of Au. As noted previously, the apparent lack of base metals enrichment may be due to the limited number of base metals analyses.

## DISTRICT-WIDE DATA SET

Geochemical data collected from district-wide sampling (table 5) consist of 67 samples (60 of which are vein samples). Figures 9-14 show anomalous values for this data, using anomalous thresholds from the Bullion Canyon data set (table 2). Molybdenum is strongly enriched in the "eastern vein area" and in the lower Bullion Canyon area. Barium data show scattered high values (as high as 27.7 percent Ba) across the district. No high geochemical values occur in the southwestern portion of the district where pervasive alteration is present. Relatively high Au, Pb, and Zn values occur in the northernmost portion of the district. Several samples collected from the Chloride Canyon fault show high values of Au, Ag, Cu, Pb, Zn, As, and Mo. A sample collected from a vein on Silver Peak shows enrichment in Au, Ag, Cu, Pb, Zn, and As.

**Table 3. Univariate statistics for the Eagle Nest data set, Antelope Range mining district. All values are in parts per million except for Hg, which is given in parts per billion.**

| Subset | | Element | n* | Mean | Maximum | Minimum** |
|---|---|---|---|---|---|---|
| Drill Hole Samples | Vein Samples | Au | 135 | .07 | .51 | .001 |
| | | Ag | 135 | 4.7 | 75.1 | .1 |
| | | Cu | 40 | 43 | 195 | 5 |
| | | Pb | 40 | 432 | 6350 | 1 |
| | | Zn | 40 | 458 | 6400 | 1 |
| | | As | 33 | 205 | 1200 | 1 |
| | | Sb | 31 | 15 | 40 | 4 |
| | | Hg | 31 | 1427 | 18,000 | 45 |
| | | Mo | 9 | 5 | 18 | 1 |
| | Non-Vein Samples | Au | 266 | .04 | .62 | .001 |
| | | Ag | 266 | 3.7 | 22.1 | .1 |
| | | Cu | 53 | 51 | 135 | 10 |
| | | Pb | 53 | 55 | 540 | 1 |
| | | Zn | 53 | 226 | 2100 | 35 |
| | | As | 15 | 159 | 500 | 30 |
| | | Sb | 15 | 14 | 30 | 6 |
| | | Hg | 15 | 1172 | 4400 | 40 |
| Surface Samples | | Au | 67 | — | — | .001 |
| | | Ag | 67 | 7.5 | 43.9 | .1 |
| | | Cu | 5 | 24 | 70 | 1 |
| | | Zn | 5 | 37 | 115 | 10 |

*n = Number of samples

** = Minimum value or lower limit of detection

## INTERPRETATION OF DATA

Geochemical data was interpreted in two ways: (1) by visual examination of the spatial distribution of anomalous values and (2) multivariate statistical analysis (factor analysis).

### Anomaly Patterns

**Base Metals-Enriched Areas**—One striking pattern on the anomaly maps (figures 9 through 14) is the clustering of base metals anomalies in the Bullion Canyon area. Areas of base metals anomalies shown in figure 16 coincide with widespread veining and hydrothermal alteration (plate 2). Base metals anomalies occur largely in vein sample data as opposed to non-vein sample data, and mostly occur below an elevation of 6200 feet, suggesting a possible vertical zonation with base metals enrichment occurring beneath precious metals enrichment. As shown in figures 9 through 13, precious metals accompanied base metals mineralization at the northern end of the EBC vein system, but elsewhere in the district, base and precious metals mineralization occurred as separate events. Limited sample results suggest that molybdenum is enriched in the area of base metals anomalies. The "eastern vein area" (figure 7) shows enrichment in base metals Mo and Ag and appears to be geochemically similar to the base metals-enriched portion of the Bullion Canyon area.

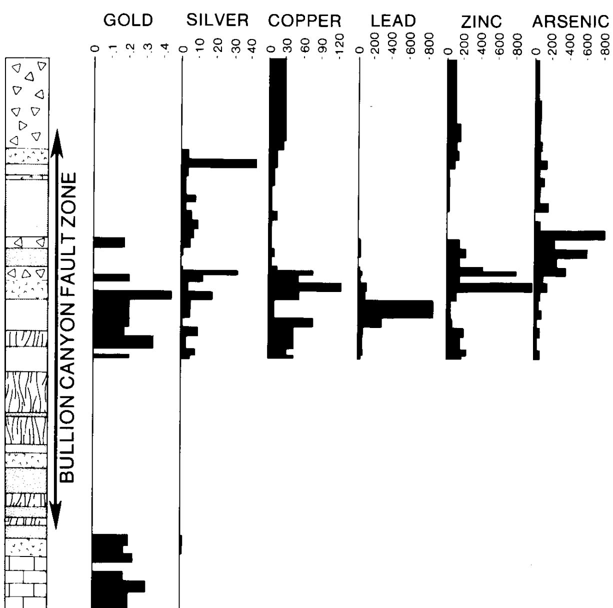


**Figure 15.** Detailed geochemical profile and lithologic log across the Bullion Canyon fault zone, as shown by drill hole 5 (figure 9). All values are in ppm. Light shaded areas are quartz veins. Dark shaded areas are calcite veins. Ash-flow tuff marked by checked pattern where not brecciated and by open triangles where brecciated. Stockwork areas hosted by mylonitized volcanic rock are shown by irregular lines. Brickwork pattern marks the Claron Formation.

**Table 4. Univariate statistics for the Bone Hollow data set, Antelope Range mining district. All values are in parts per million except for Hg, which is given in parts per billion.**

| Subset | Element | n* | Mean | Maximum | Minimum** |
|---|---|---|---|---|---|
| Drill Hole Samples | Au | 50 | .08 | .79 | .001 |
| | Ag | 50 | .6 | 10.6 | .1 |
| | Cu | 22 | 39 | 115 | 1 |
| | Pb | 22 | 112 | 600 | 1 |
| | Zn | 22 | 272 | 1100 | 1 |
| | As | 22 | 106 | 400 | 40 |
| | Sb | 22 | 9 | 14 | 5 |
| | Hg | 22 | 25 | 50 | 10 |
| Surface Samples | Au | 97 | .41 | 7.54 | .001 |
| | Ag | 97 | 6.5 | 51.4 | .1 |

*n = Number of samples

** = Minimum value or lower limit of detection

**Silver-Rich Vein Systems**—The Eagle Nest, Trench Hill, Blair, and northern tip of the EBC vein systems are strongly enriched in Ag relative to Au. These Ag-enriched areas are characterized by Au to Ag ratios ranging from .06 to .08 and contain Ag values as great as 310 ppm (9.04 oz/ton). The Ag-enriched areas form a linear belt that trends northwesterly across the district (the "silver belt," figure 16). The extent of base metals-enrichment associated with this Ag-rich trend is not well defined by existing data.

**Precious Metals-Enriched Systems**—The Bone Hollow vein system shows enrichment in both Au and Ag and contains 19 of the 35 Au anomalies located in the central part of the district. Au to Ag ratios have an average value of .15, twice as high as the district average. Anomalous Au values from the Bone Hollow system define a zone of relative Au enrichment lying parallel to, and just west of, the "silver belt" described above (figure 16). Another area of Au enrichment, with associated enrichment in Ag and base metals, occurs at the northern tip of the EBC vein system. A lateral zonation is thus suggested by the parallel arrangement of these geochemically distinct vein systems.

### Factor Analysis

Factor analysis is a multivariate statistical procedure used to show interrelationships between variables in a data set. With geochemical data, factor analysis creates new variables (called factors) defined in terms of original variables (elemental analyses). The goal is to represent the data set by a smaller number of mutually-independent variables while preserving as much of the total variance of the data set as possible. Factors produced by this procedure typically reflect geochemical processes. R-mode factor analysis and the varimax rotation procedure (Kaiser, 1958) were used to produce the factor models discussed below. Joreskog and others (1976) discuss the factor analysis method.

Factor analysis results are best interpreted in terms of ore and gangue mineralogy and the paragenetic sequence. It is assumed that the distributions of elements used in the geochemical study largely reflect primary dispersion caused by hypogene mineralization process. To aid in the interpretation, the mineralogy of hypogene mineralization stages was used to derive anticipated geochemical "enrichment suites" (table 6). The following discussion presents factor analysis results for each vein system for which sufficient geochemical data exists (table 7).

Factor analysis for the Bullion Canyon area produced a three-factor model explaining 80 percent of the variance of the vein sample data set. The first two factors mimic the two stages of sulfide mineral paragenesis: factor 1 (Cu+Pb+Zn) represents base metals mineralization (stage 1) and factors 2 (Au+Ag) and 3 (As+Cu) represent stage II (silver sulfosalt mineralization). These results strongly support the paragenetic sequence. Of interest is the grouping of Au and Ag in factor 2 and their correlation coefficient of .42 (threshold = .14). This suggests that, in the Bullion Canyon area, Au enrichment was associated with the silver sulfosalt stage. No significant correlation between Au and Ag exists in data from the rest of the district. The lack of association between Ag and As as predicted from the mineralogy (table 6) may indicate that supergene processes remobilized As and possibly Ag as well.

Non-vein samples from the Bullion Canyon area produced a slighly different factor model. Factor 1 for this set corresponds to stage Ib mineralization and factor 2 to stage II. This is the only data set that shows the complete stage II geochemical association of Ag+As+Cu as predicted from the mineralogy. As opposed to vein samples, no significant correlation (coefficient = .13, threshold = .27) exists between Au and Ag.

Factor analysis results for the Bone Hollow vein system show that As, Cu, Pb, and Zn form the first factor. This raises the possibility of an As-bearing sulfide, possibly arsenical pyrite, as part of stage I mineralization in this area. Au and Ag mineralization evidently occurred as separate events, as shown by their correlation coefficient of -0.06 (threshold = 0.17).

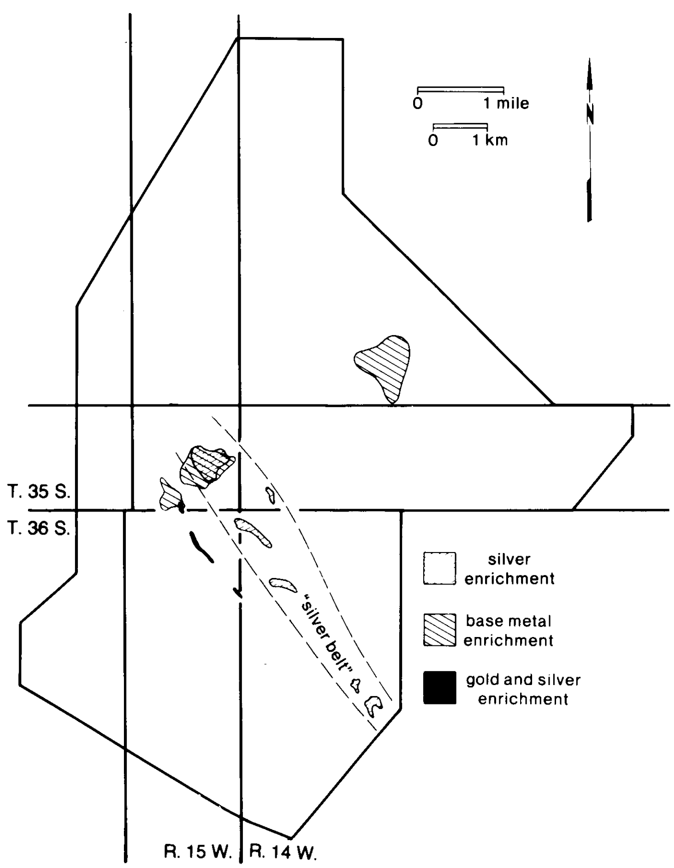


**Figure 16.** Simplified geochemical map showing areas characterized by base metals enrichment, silver enrichment, and gold and silver enrichment. Dashed lines delineate zone of silver enrichment ("silver belt").

**Table 5. Univariate statistics for the district-wide data set, Antelope Range mining district. All values are in parts per million.**

| Element | n* | Mean | Maximum | Minimum** |
|---|---|---|---|---|
| Au | 67 | .24 | 1.91 | .001 |
| Ag | 67 | 18.7 | 310 | .1 |
| Cu | 67 | 2889 | 49,000 | 1 |
| Pb | 67 | 6525 | 110,000 | 10 |
| Zn | 67 | 3331 | 65,400 | 6 |
| As | 67 | 187 | 1940 | 1 |
| Sb | 67 | 25 | 133 | .5 |
| Mo | 67 | 34 | 377 | 1 |
| W | 67 | 18 | 180 | 1 |
| Ba | 67 | 10,396 | 277,000 | 25 |

*n = Number of samples

** = Minimum value or lower limit of detection

**Table 6. Relationships between hypogene mineralization stages, mineralogy, and predicted geochemical enrichments, Bullion Canyon area, Antelope Range mining district. Minor components given in parenthesis.**

| Hypogene Mineral-ization Stage | | Pertinent Mineralogy | Predicted Geochemical Enrichment Suite |
|---|---|---|---|
| Base-metal | Ia | Galena, chalcopyrite | Pb+Cu |
| Stage | Ib | Galena, Sphalerite, Barite (chalcopyrite) | Pb+Zn+Ba(+Cu) |
| Silver Sulfosalt Stage | II | Pearceite, Tennantite, Stromeyerite, Proustite | Ag+As+Cu |
| Barren Stage | III | Barite | Ba |

Vein data from the Eagle Nest area show the presence of stage I mineralization, represented by factor 1 (Cu+Pb+Zn). Ag, As, and Au appear to have independent distributions. Pb and Zn in this data set show the strongest correlation observed between any two elements in the district, with a correlation coefficient of 0.93 (threshold = 0.17). Non-vein data produced a much different factor model. In this set Pb, Zn, and As form the first factor, again suggesting the presence of an arsenic-bearing phase (arsenical pyrite ?) associated with stage I mineralization. Au and Ag comprise the second factor.

District-wide data, analyzed by the neutron activation method, show interesting results. In this factor model, Cu and Pb form the first factor, representing the stage Ia mineralization event. Factor 2 consists of Au and As, a common elemental association in precious metals-bearing hot springs systems, and may represent gold mineralization deposited in such an environment. Recognition of this elemental association in the district-wide data set resulted from the use of the highly sensitive neutron activation analysis. Factor 3 of the model consists of W, Mo, and As, another common type of hot springs

**Table 7. Factor analysis results, Antelope Range mining district.**

| Data Set | | n* | r** | Variables used in analysis | Numbers of factors selected | Percent variance explained*** | Factors**** |
|---|---|---|---|---|---|---|---|
| Bullion Canyon | Vein | 199 | .14 | Au Ag<br>Cu Pb<br>Zn As | 3 | 80 | 1. Cu (.71) + Pb (.87) + Zn (.92)<br>2. Au (.84) + Ag (.84)<br>3. As (.95) + Cu (.44) |
| Bullion Canyon | Non-Vein | 51 | .27 | Au Ag<br>Cu Pb<br>Zn As | 3 | 80 | 1. Pb (.95) + Zn (.97)<br>2. Cu (.94) + Ag (.82) + As (.58)<br>3. Au (.99) |
| Bone Hollow | | 124 | .17 | Au Ag<br>Cu Pb | 3 | 80 | 1. Cu (.88) + Pb (.83) + Zn (.91) + As (.68)<br>2. Au (.99) +<br>3. Ag (.98) + |
| Eagle Nest | Vein | 135 | .16 | Au Ag<br>Cu Pb<br>Zn As | 4 | 91 | 1. Cu (.53) + Pb (.96) + Zn (.97)<br>2. Ag (.99) +<br>3. As (.97) +<br>4. Au (.93) + Cu (.47) |
| Eagle Nest | Non-Vein | 266 | .12 | Au Ag<br>Cu Pb<br>Zn As | 3 | 81 | 1. Pb (.93) + Zn (.79) + As (.92)<br>2. Au (.82) + Ag (.82)<br>3. Cu (.96) + Zn (.46) |
| District-Wide (vein samples only) | | 60 | .25 | Au Ag<br>Cu Pb<br>Zn As<br>Sb Mo<br>W Ba | 7 | 86 | 1. Cu (.91) + Pb (.83)<br>2. Au (.94) + As (.67)<br>3. W (.88) + Mo (.56) + As (.60)<br>4. Ba (.99) +<br>5. Ag (.98) +<br>6. Sb (.96) +<br>7. Zn (.95) + |
| Combined Bullion Canyon and District-wide Data Set (Vein Samples Only) | | 259 | .12 | Au Ag<br>Cu Pb<br>Zn As<br>Calcite<br>Quartz<br>Barite<br>Chalcedony | 7 | 83 | 1. Cu (.92) + Pb (.83)<br>2. Zn (.49) + Calcite (.92)<br>3. Au (.79) + Ag (.74)<br>4. Zn (.67) + Barite (.89) + Pb (.31)<br>5. Quartz (.99)<br>6. As (.98)<br>7. Chalcedony (.92) |

*n = Number of samples

**r = Threshold value for significant correlation at the 95% confidence level based on size of population (Snedecor and Cochran, 1980).

*** = Percent variance of the original data set explained by the given factor model.

**** = Numbers in parenthesis are the correlation coefficients between the original variable and the factors. Factors listed were derived from R-mode factor analysis using the Varimax rotation criteria (see text).

association (Berger and Silberman, 1985). The remaining factors are single-element factors indicating independent behavior of these elements.

Mineralogical data were included in a factor model for the combined Bullion Canyon and district-wide data sets (table 7). This mineralogical data consists of visual estimates of the percentages of quartz, calcite, chalcedony, and barite present in vein samples. Factor 1 of this model consists of Cu+Pb, representing stage Ia hypogene mineralization. Factor 2 consists of Zn+calcite. This factor may represent an aspect of stage Ib hypogene mineralization (coprecipitation of sphalerite and calcite) or may be a product of supergene processes. Factor 3 is the precious metals mineralization factor as noted above in the discussion of the Bullion Canyon data. Factor 4 represents stage Ib mineralization, with Pb only weakly loaded into this factor. The remaining factors are single-element factors (table 7). Of interest in this model is the failure of quartz and chalcedony to show any correspondence with elemental data. This underscores the observation that vein mineralogy is not an accurate guide to geochemical enrichment.

## DESCRIPTION OF WORKINGS

Plate 2 shows the location of mine workings and prospect pits in the Antelope Range district. Workings consist of many (small) shafts, adits, and prospect pits. Maps of the three longest adits are shown in figure 17; see plate 2 for location. These adits have a total passable length of 965 feet (294 m). A total of 29 vertical to inclined shafts occur in the district, most of which are less than 50 feet (15 m) in depth. A great number of prospect pits and trenches also exist. The total estimated length of mine workings in the Antelope Range district is 2200 feet (670 m). In comparison to other districts, workings in the Antelope Range district are minor.

## CONCLUSIONS

### GENESIS OF MINERALIZATION

Mineralization in the Antelope Range district may be classified as the epithermal, base and precious metals, vein type (Buchanan, 1981), the quartz-adularia (low sulfur) bonanza-type of Berger and Eimon (1983), or the adularia-sericite type of Heald and others (1986). Mineralized veins in the Antelope Range district are similar in many respects to the deposit currently being mined at the Escalante silver mine (Fitch and Brady, 1982). A genetic model of mineralization in the Antelope Range district is presented below. Elements discussed in the model are depicted in figure 18.

1. Northwest-striking, extension-related faulting (Middle to Late Miocene) in the area largely preceded mineralization and alteration. Faults produced during this deformation host all known occurrences of mineralized veins. Neogene extensional faulting was the structural preparation that allowed the circulation of hydrothermal fluids.
2. Eruption of rhyolitic flows and intrusion of possible subvolcanic rocks occurred 8.5 to 8.4 Ma.
3. Heat derived from the emplacement of rhyolitic magmas induced a hydrothermal system in the surrounding host rocks. Extensional structures served as conduits for rising, dominantly meteoric, hydrothermal solutions.
4. Structurally controlled alteration took place as hydrothermal solutions diffused outwards from conduit structures, depositing silica and altering plagioclase and glass to kaolinite and other clays. Early silica precipitation may have sealed conduit walls in sedimentary rocks, preserving host rocks from extensive alteration.
5. Boiling occurred at the top of the hydrothermal system at a depth greater than 460 feet (140 m) beneath the prevailing water table.
6. The main phase of boiling produced the earlier stage I mineralization, consisting of base metals deposition in a quartz, calcite, and barite gangue assemblage.
7. Later, a second boiling event initiated stage II precipitation of quartz and silver sulfosalts, overprinting stage I mineralization. This event was responsible for silver mineralization in the "silver belt."
8. It is speculated that a third mineralizing event occurred that produced the dominantly chalcedonic veins and relatively gold-rich mineralization observed in the Bone Hollow vein system. Alternatively, mineralization in the Bone Hollow system and the "silver belt" may have occurred simultaneously. The Bone Hollow system is geochemically and mineralogically similar to the "root zone" of a hot springs system.
9. "Silica flooding" of the Little Pinto fault produced the chalcedonic Little Pinto vein and adjacent areas of extreme silicification. Silica flooding, locally subjacent kaolinitic alteration, and pervasive argillization may represent the upper (hot springs) portions of a hydrothermal system. The timing of this event relative to the three mineralizing events described above is uncertain.
10. Supergene alteration destroyed many of the primary sulfides in the district and erosion produced the present level of exposure.

### MINERAL POTENTIAL

Potential exists for the discovery of three types of mineral deposits in the Antelope Range district: (1) epithermal, base and precious metals vein and stockwork deposits, (2) disseminated precious metals deposits, and (3) manto replacement deposits. A remote potential also exists for the discovery of a deeply buried porphyry Cu-Mo mineral occurrence.

#### Epithermal Vein and Stockwork Deposits

Vein-type precious metals deposits have the highest probability for discovery in the Antelope Range district. An estimate of the potential size of such deposits may be gained by making a comparison to the geologically similar Escalante silver mine. As of 1983, proven ore reserves at the mine totaled 1.67 million short tons averaging 10.37 oz/ton silver (Burger, 1984), and as of 1985, total silver production exceeded 9 million ounces. The

Escalante ore body has a strike length of approximately 3500 feet (1100 m), extends to a depth of over 800 feet (250 m), and averages 20 feet (6 m) in width. The dimensions of the Escalante vein exceed the mapped surface expression of any vein in the Antelope Range district. However, the full extent of the Escalante vein was known only after extensive exploration and its surface expression is not unlike many veins in the Antelope Range district. The Escalante deposit differs geochemically from mineralized veins in the Antelope Range district in that it contains less copper (less than 500 ppm), lower values of lead and zinc, and substantially more fluorine.

Grade-tonnage models provide another means of estimating the size of potential vein-type mineral deposits in the Antelope Range district. These models compiled by Cox and Singer (1986) show a probabilistic relationship between the size and grades of many deposit types. One may consider potential precious metals vein deposits in the Antelope Range district (and the Escalante vein) to be silver-rich versions of the Creede-type deposits of Cox and Singer who have plotted the cumulative proportion of well-explored deposits of this type versus their tonnage and ore grades. Their results show that the median (50th percentile) size of a Creede-type deposit is 1.5 million short tons with median cutoff grades of 3.8 oz/ton silver and 0.04 oz/ton gold (slightly smaller than the Escalante deposit).

Within the Antelope Range district, the West Blair vein (figures 7 and 8) has the highest potential for discovery of a silver-rich, epithermal vein deposit. This vein has a cumulative strike length of 2000 feet (610 m) and is host to the greatest density of silver anomalies in the district. Although one hole was drilled near the West Blair vein, it is uncertain if the vein was penetrated. A second vein target is the Trench Hill area (figure 7), which contains the highest silver value in the district (over 9 oz/ton). Several relatively long and continuous veins occur there and previous exploration was limited. A third target is the nearly unexplored EBC system (figure 7), which is geochemically attractive because of the presence of both gold and silver anomalies. A fourth target, the Bone Hollow system, was partially explored (yielding discouraging results) but may be of interest because of its relative high gold content. A

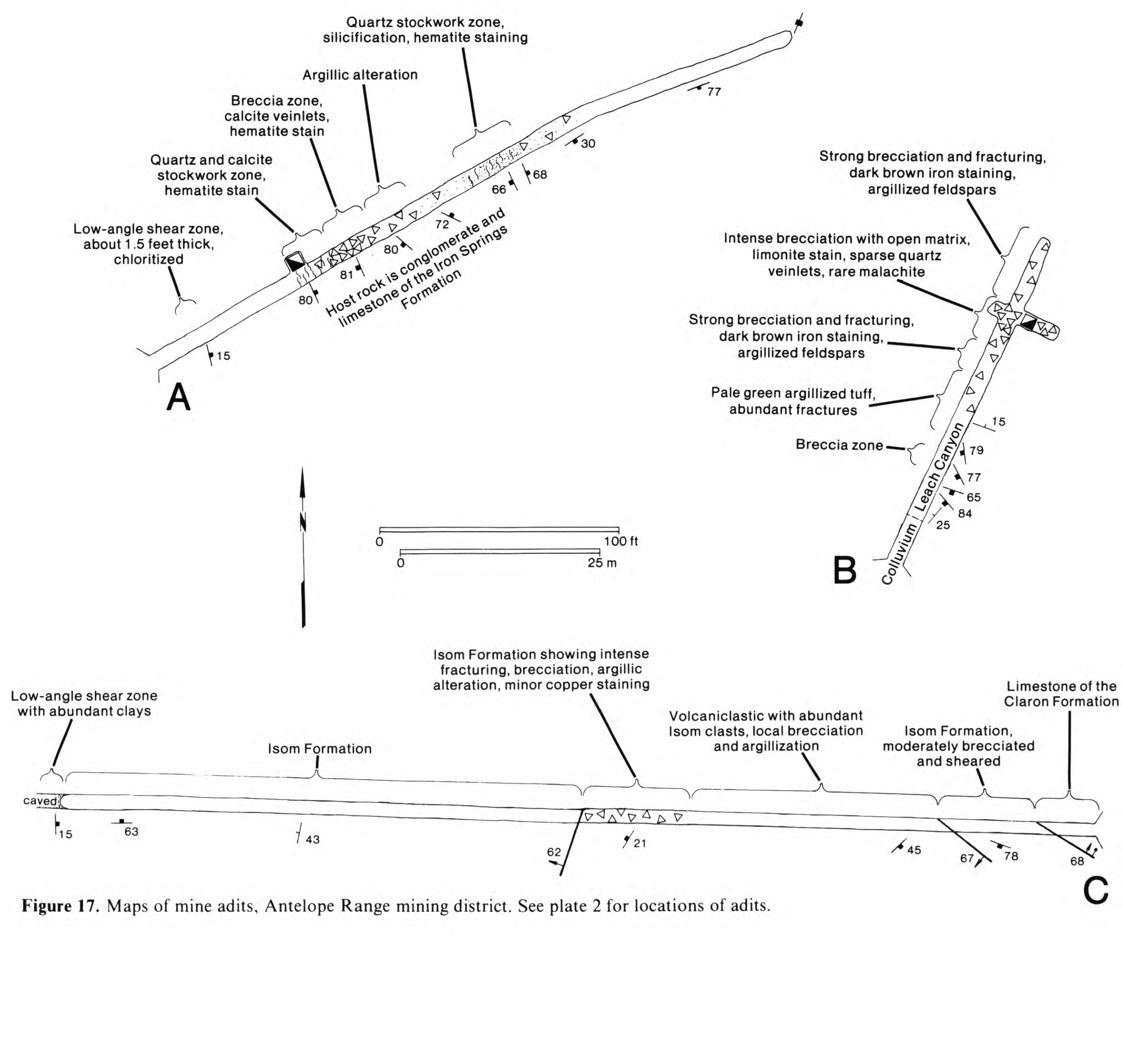


**Figure 17.** Maps of mine adits, Antelope Range mining district. See plate 2 for locations of adits.

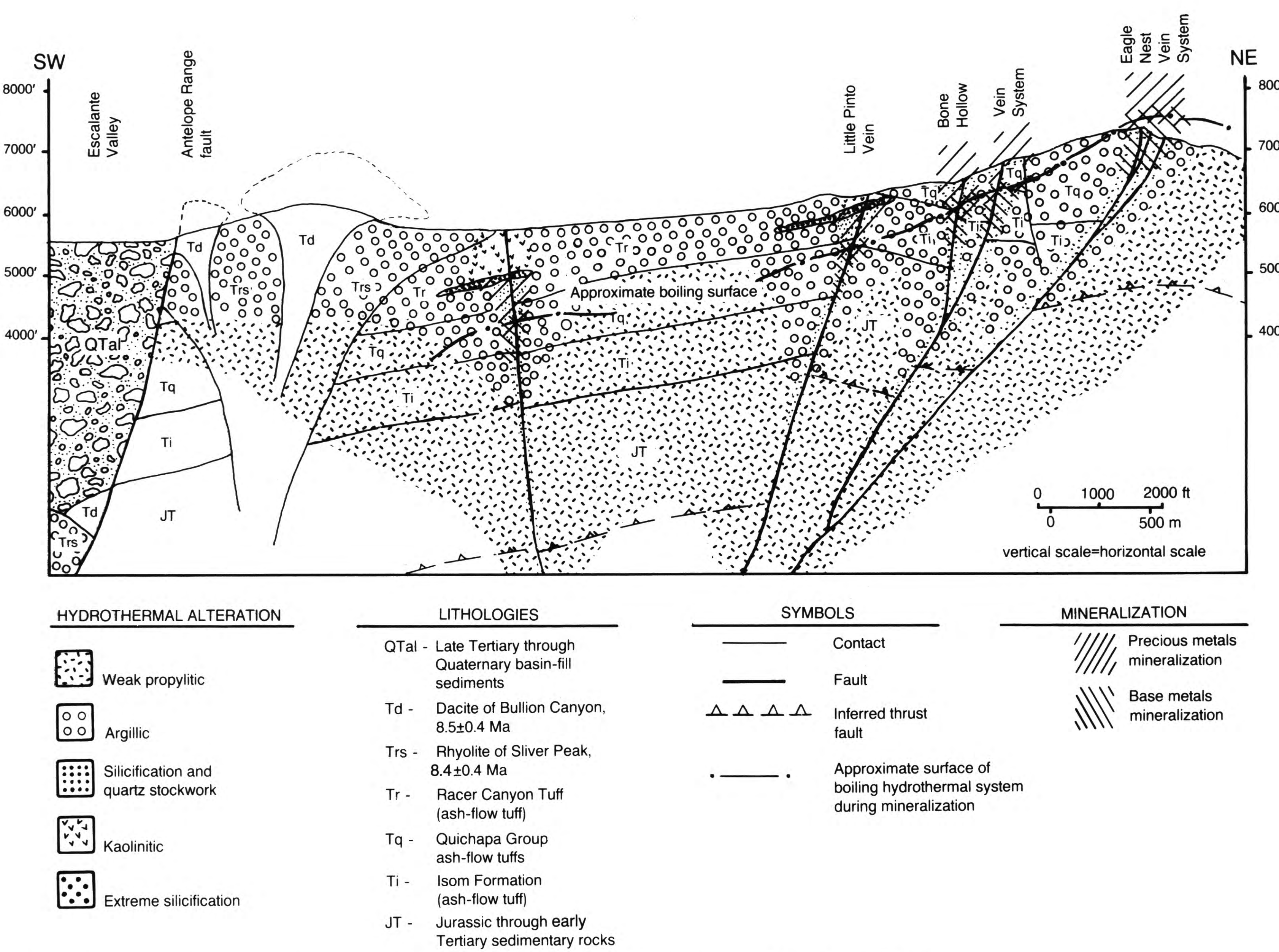


**Figure 18.** Diagrammatic cross section showing the relationships between hydrothermal alteration zones and mineralization. Line of cross section coincides with cross section A-A′ shown on plate 1. Named vein systems correspond to those shown on plate 2.

final vein target, the Little Pinto vein, remains unexplored and could represent the top of a mineralizing system. Of ten samples collected from the Little Pinto vein, the highest precious metals values obtained were 1.4 ppm Au and 22 ppm Ag.

### Related Mineralization

Conceptual potential exists for disseminated precious metals mineralization in areas adjacent to veins where such mineralization might be stratigraphically controlled by the Claron-Isom contact. Disseminated mineralization may also be present adjacent to the Little Pinto vein where self-sealing of the densely silicified interbed of the Racer Canyon Tuff may have occurred (figure 18). Repeated episodes of self-sealing, hydrothermal brecciation and precious metals deposition may have produced a disseminated deposit. Manto replacement mineralization may have occurred where carbonate rocks (especially the Homestake Limestone Member of the Carmel Formation) lie adjacent to mineralized veins. Such deposits would presumably be composed of nearly massive bodies of lead-, zinc-, silver-, and copper-bearing sulfides. Since manto deposits typically flank calcalkaline plutons and often show evidence of a significant contribution of magmatic fluids (Beaty and others, 1986), the likelihood of such deposits occurring in the Antelope Range district is minimal.

## ACKNOWLEDGMENTS

The authors would like to thank Mr. William Crowl of the Homestake Mining Company and Mr. Neil Muncaster, former exploration manager of the Tenneco Minerals Company, for access to data that greatly enhanced this study. Thanks also are due to L.P. James, J.M. Ballantyne, L.F. Hintze, and H.H. Doelling for their thoughtful reviews of the manuscript.

## REFERENCES

Anderson, J.J., Rowley, P.D., Fleck, R.J., 1975, Cenozoic stratigraphy of southwestern High Plateaus of Utah, *in* J.J., Rowley, P.D., Fleck, R.J., and Nairn, A.E.M., eds., 1975, Cenozoic Geology of Southwestern High Plateaus of Utah: Geological Society of America Special Paper 160, p. 1-52.

Anon., 1901, Salt Lake Mining Review, May 30, page 15, column 3.

Anon., 1913, Salt Lake Mining Review, July 30, page 29, column 1.

Armstrong, R.L., 1968, Sevier orogenic belt in Nevada and Utah: Geological Society America Bulletin, v. 79, p. 429-458.

Beaty, D.W., Cunningham, C.G., Rye, R.O., Steven, T.A., and Gonzalez-Urien, Eliseo, 1986, Geology and geochemistry of the Deer Trail Pb-Zn-Ag-Au-Cu manto deposits, Marysvale district, west-central Utah: Economic Geology, v. 81, no. 8, p. 1932-1952.

Best, M.G., 1986, Tertiary geology of the area between Milford, Utah and Pioche, Nevada, *in* Griffen, D.T., and Phillips, W.R., eds., Thrusting and Extensional Structures and Mineralization in the Beaver Dam Mountains, Southwestern Utah: Utah Geological Association Publication 15, p. 77-86.

Berger, B.R., and Eimon, P.I., 1983, Conceptual models of epithermal precious-metals deposits, *in* Shanks, W.C., ed., Cameron Volume on Unconventional Mineral Deposits: Society of Mining Engineers, New York, p. 191-205.

Berger, B.R., and Silberman, M.L., 1985, Relationships of trace-metal patterns to geology in hot-spring-type precious-metal deposits, *in* Berger, B.R., and Bethke, P.M., eds., Geology and Geochemistry of Epithermal Systems: Society of Economic Geologists, Reviews in Economic Geology, v. 2, p. 233-247.

Blank, H.R., Jr., 1959, Geology of the Bull Valley district, Washington County, Utah: Seattle, University of Washington, Ph.D. dissertation, 177p.

Blank, H.R., Jr., and Mackin, J.H., 1967, Geologic interpretation of an aeromagnetic survey of the Iron Springs district, Utah: U.S. Geological Survey Professional Paper 516-B, 14 p.

Buchanan, L.J., 1981, Precious-metal deposits associated with volcanic environments in the southwest, *in* Dickinson, W.R., and Payne, W.D., eds., Relations of Tectonics to Ore Deposits in the South Cordillera: Arizona Geological Society Digest, V. XIV, p. 237-262.

Bullock, K.C., 1970, Iron deposits of Utah: Utah Geological and Mineral Survey Bulletin 88, 101 p.

Bullock, K.C., 1973, Geology and iron deposits of the Iron Springs district, Iron County, Utah: Brigham Young University Geology Studies, v. 20, pt. 1, p. 27-63.

Burger, J.R., 1984, Ranchers end-slices Escalante silver deposit: Engineering and Mining Journal, v. 185, no. 1, p. 48-53.

Clement, M.D., 1980, Escalante Desert: Heatflow and geothermal assessment of the Oligocene/Miocene volcanic belt in southwestern Utah: Salt Lake City, University of Utah, M.S. thesis, 118 p.

Cook, E.F., 1957, Geology of the Pine Valley Mountains: Utah Geological and Mineral Survey Bulletin 58, 111 p.

Cook, E.F., 1965, Stratigraphy of Tertiary volcanic rocks in eastern Nevada: Nevada Bureau of Mines Report, no. 11, 61 p.

Cook, K.L., and Hardman, Elwood, 1967, Regional gravity survey of the Hurricane fault area and Iron Springs district, Utah: Geological Society of America Bulletin, v. 78, p. 1063-1076.

Cox, D.P., and Singer, D.A. eds., 1986, Mineral deposit models: U.S. Geological Survey Bulletin 1693, 379 p.

Ekren, E.B., Bucknam, R.C., Carr, W.J., Dixon, G.L. and Quinlivan, W.D., 1976, East-trending structural lineaments in central Nevada: U.S. Geological Survey Professional Paper 986, 16 p.

Ekren, E.B., Orkild, P.P., Sargent, K.A., and Dixon, G.L., 1977, Geologic map of Tertiary rocks, Lincoln County Nevada: U.S. Geological Survey Miscellaneous Geologic Investigations Map I-1041.

Fitch, D.C., and Brady, M.W., 1982, Geology of the Escalante Silver Mine, Utah: Northwest Mining Association 88th Annual Convention, Spokane, Washington (reprint of presentation).

Fournier, R., 1978, Silver Peak project, Iron County, Utah: unpublished report, Tenneco Minerals Company.

Haas, J.L., Jr., 1971, The effect of salinity on the maximum thermal gradient of a hydrothermal system at hydrostatic pressure: Economic Geology, v. 66, p. 940-946.

Heald, P., Hayba, D.O., and Foley, N.K., 1986, Comparative anatomy of volcanic-hosted epithermal deposits: Acid-sulfate and adularia-sericite types: Economic Geology, v. 82, no. 1, p. 1-26.

Hedenquist, J.W., and Henley, R.W., 1985, The importance of $CO_2$ on freezing point measurements of fluid inclusions: evidence from active geothermal system and implications for epithermal ore deposition: Economic Geology, v. 80, p. 1379-1405.

Hintze, L.F., 1986, Stratigraphy and strucure of the Beaver Dam Mountains, southwestern Utah, *in* Griffen, D.T., and Phillips, W.R., eds., Thrusting and Extensional Structures and Mineralization in the Beaver Dam Mountains, Southwestern Utah: Utah Geological Association Publication 15, p. 1-36.

Huntley, D.B., 1885, The mining industries of Utah: U.S. 10th Census, v. 13, p. 476-477.

Johnson, B.T., 1983, Depositional environment of the Iron Springs Formation, Gunlock, Utah: Brigham Young University Geology Studies, v. 31, pt. 1, p. 29-46.

Joreskog, K.G., Klovan, J.E., and Reyment, R.A., 1976, Geological factor analysis: New York, Elsevier Scientific Publishing Company, 178 p.

Kaiser, H.F., 1958, The varimax criterion for analytic rotation in factor analysis: Phychometrika, v. 23, p. 187-200.

Kamilli, R.J., and Ohmoto, H., 1977, Paragenesis, zoning, fluid inclusion, and isotopic studies of the Finlandia Vein, Colqui district, central Peru: Economic Geology, v. 72, p. 950-982.

Leith, C.K., and Harder, E.C., 1908, Iron ores of the Iron Springs district, southern Utah: U.S. Geological Survey Bulletin 338, 102 p.

Lewis, A.E., 1958, Geology and mineralization connected with the intrusion of a quartz monzonite porphyry, Iron Mountain, Iron Springs district, Utah: Pasadena, California Institute of Technology, Ph.D. dissertation, 75 p.

Mackin, J.H., 1947, Some structural features of the intrusions in the Iron Springs district: Utah Geological Society Guidebook to the Geology of Utah, no. 2, 62 p.

Mackin, J.H., 1954, Relationship between deformation and igneous activity in the Colorado Plateau-Basin and Range transition zone in southwestern Utah [abs.]: Geological Society of America Bulletin, v. 66, no. 12, pt. 2, p. 1592.

Mackin, J.H., 1960, Structural significance of Tertiary volcanic rocks in southwestern Utah: American Journal of Science, v. 258, p. 81-131.

Mackin, J.H., 1968, Iron ore deposits of the Iron Springs district, southwestern Utah, *in* Ore Deposits of the United States, 1933-1967 (Graton-Sales volume), v. 2: New York, American Institute of Mining, Metallurgical and Petroleum Engineers, p. 992-1019.

Mackin, J.H., Nelson, W.H., and Rowley, P.D., 1976, Geologic map of the Cedar City NW quadrangle, Iron County, Utah: U.S. Geological Survey Geologic Quadrangle Map GQ-1295.

Mackin, J.H., Nelson, W.H., and Rowley, P.D., 1977, Geologic map of the Desert Mound quadrangle, Iron County, Utah: unpublished mapping.

McIntosh, W.S., 1987, Geology and mineralization of the Bullion Canyon area, Iron County, Utah: Fort Collins, Colorado State University, M.S. thesis.

Nash, J.T., 1976, Fluid inclusion petrology—data from porphyry copper deposits and applications to exploration: U.S. Geological Survey Professional Paper 907-D, 16 p.

Noble, D.C., and McKee, E.H., 1972, Description and K-Ar ages of volcanic units of the Caliente volcanic field, Lincoln County, Nevada, and Washington County, Utah: Isochron/West, no. 5, p. 17-24.

Pe, Win, and Cook, K.L., 1980, Gravity survey of the Escalante Desert and vicinity, in Iron and Washington Counties, Utah: Earth Science Laboratory/ University of Utah Research Institute Report No. DOE/ID/12079-14, 169 p.

Ratté, C.A., 1963, Rock alteration and ore genesis in the Iron Springs-Pinto mining district, Iron County, Utah: Tucson, University of Arizona, Ph.D. dissertation, 222 p.

Roedder, E., 1984, Fluid inclusions: Mineralogical Society of America, Reviews in Mineralogy, v. 12, 644 p.

Rowley, P.D., and Barker, D.S., 1978, Geology of the Iron Springs mining district, Utah, *in* Shawe, D.R., and Rowley, P.D., eds., International Association on Genesis of Ore Deposits, Guidebook to Mineral Deposits of Southwestern Utah: Utah Geological Association Publication 7, p. 49-58.

Rowley, P.D., Steven, T.A., Anderson, J.J., and Cunningham, C.G., 1979, Cenozoic stratigraphic and structural framework of southwestern Utah: U.S. Geological Survey Professional Paper 1149, 22 p.

Shawe, D.R., and Stewart, J.H., 1976, Ore deposits as related to tectonics and magmatism, Nevada and Utah: American Institute of Mining, Metallurgical, and Petroleum Engineers Transactions, v. 260, p. 225-232.

Shubat, M.A. and Siders, M.A., 1988, Geologic map of the Silver Peak quadrangle, Iron County, Utah: Utah Geological and Mineral Survey Map 108.

Siders, M.A., 1985, Geology of the Beryl Junction quadrangle, Iron County, Utah: Utah Geological and Mineral Survey Map 85.

Siders, M.A., and Shubat, M.A., 1986, Stratigraphy and structure of the northern Bull Valley Mountains and Antelope Range, Iron County, Utah, *in* Griffen, D.T., and Phillips, W.R., eds., Thrusting and Extensional Structures and Mineralization in the Beaver Dam Mountains, Southwestern Utah: Utah Geological Association Publication 15, p. 87-102.

Smith, R.B., 1978, Seismicity, crustal structure, and intraplate tectonics of the interior of the western Cordillera, *in* Smith, R.B., and Eaton, G.P., eds., Cenozoic Tectonics and Regional Geophysics of the Western Cordillera: Geological Society of America Memoirs 152, p. 111-144.

Snedecor, G.W., and Cochran, W.G., 1980, Statistical methods (7th ed): Ames, Iowa, Iowa State University Press, 507 p.

Steven, T.A., and Morris, H.T., 1984, Mineral resource potential of the Richfield 1° x 2° quadrangle, west central Utah: U.S. Geological Survey Open-File Report 84-521, 53 p.

Tobey, E.F., 1977, Geology of the Bull Valley intrusive-extrusive complex and genesis of the associated iron deposits: Eugene, University of Oregon, Ph.D. dissertation, 244 p.

Wernicke, B.P., 1981, Low-angle normal faulting in the Basin and Range Province: Nappe tectonics in an extending orogen: Nature, v. 291, p. 645-648.

Wernicke, B.P., 1985, Uniform-sense normal simple shear of the continental lithosphere: Canadian Journal of Earth Science, v. 22, p. 108-125.

Wernicke, B.P., in press, Basin and Range extensional tectonics, *in* Burchfiel, et al., eds., The Cordilleran Orogen: Conterminous U.S.: Geological Society of America, DNAG series.

Williams, P.L., 1967, Stratigraphy and petrography of the Quichapa Group, southwestern Utah and southeastern Nevada: Seattle, University of Washington, Ph.D. dissertation, 139 p.

Zoback, M.L., Anderson, R.E., and Thompson, G.A., 1981, Cenozoic evolution of the state of stress and style of tectonism of the Basin and Range Province of the western United States: Philosophical Transactions of the Royal Society of London, Series A, v. 300, p. 407-434.

STATE OF UTAH
DEPARTMENT OF NATURAL RESOURCES
UTAH GEOLOGICAL AND MINERAL SURVEY

Published and sold by
UTAH GEOLOGICAL AND MINERAL SURVEY
Genevieve Atwood, Director
606 Black Hawk Way
Salt Lake City, Utah 84108



# GEOLOGIC MAP OF THE ANTELOPE RANGE MINING DISTRICT, IRON COUNTY, UTAH

by
Michael A. Shubat[1] and W. Skip McIntosh[2]
[1]Utah Geological and Mineral Survey
[2]Colorado State University, Fort Collins, Colorado

1988

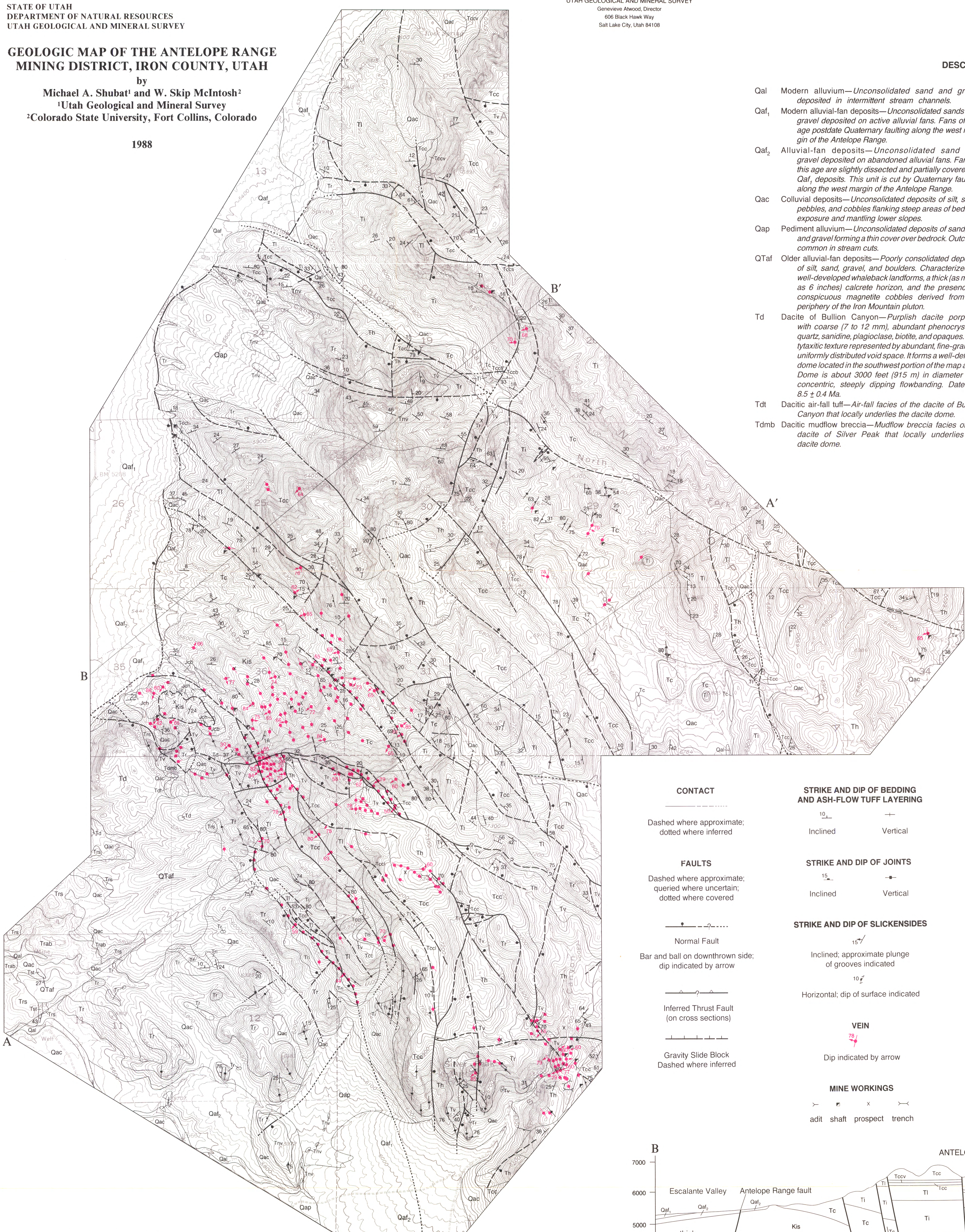

## DESCRIPTION OF MAP UNITS

**Qal** Modern alluvium—*Unconsolidated sand and gravel deposited in intermittent stream channels.*

**Qaf$_1$** Modern alluvial-fan deposits—*Unconsolidated sands and gravel deposited on active alluvial fans. Fans of this age postdate Quaternary faulting along the west margin of the Antelope Range.*

**Qaf$_2$** Alluvial-fan deposits—*Unconsolidated sand and gravel deposited on abandoned alluvial fans. Fans of this age are slightly dissected and partially covered by Qaf$_1$ deposits. This unit is cut by Quaternary faulting along the west margin of the Antelope Range.*

**Qac** Colluvial deposits—*Unconsolidated deposits of silt, sand, pebbles, and cobbles flanking steep areas of bedrock exposure and mantling lower slopes.*

**Qap** Pediment alluvium—*Unconsolidated deposits of sand, silt, and gravel forming a thin cover over bedrock. Outcrops common in stream cuts.*

**QTaf** Older alluvial-fan deposits—*Poorly consolidated deposits of silt, sand, gravel, and boulders. Characterized by well-developed whaleback landforms, a thick (as much as 6 inches) calcrete horizon, and the presence of conspicuous magnetite cobbles derived from the periphery of the Iron Mountain pluton.*

**Td** Dacite of Bullion Canyon—*Purplish dacite porphyry with coarse (7 to 12 mm), abundant phenocrysts of quartz, sanidine, plagioclase, biotite, and opaques. Diktytaxitic texture represented by abundant, fine-grained, uniformly distributed void space. It forms a well-defined dome located in the southwest portion of the map area. Dome is about 3000 feet (915 m) in diameter with concentric, steeply dipping flowbanding. Dated at 8.5 ± 0.4 Ma.*

**Tdt** Dacitic air-fall tuff—*Air-fall facies of the dacite of Bullion Canyon that locally underlies the dacite dome.*

**Tdmb** Dacitic mudflow breccia—*Mudflow breccia facies of the dacite of Silver Peak that locally underlies the dacite dome.*

**Trs** Rhyolite of Silver Peak—*Purplish-gray rhyolite to trachyte porphyry flow rocks with glassy matrix and medium-grained (3 mm) phenocrysts of quartz, sanidine, plagioclase, biotite, and trace opaques. Irregular vesicles (5 mm in diameter) comprise up to 17 percent of the rock. Consists of several coalescing volcanic domes located in the west- central portion of the map area. Dated at 8.4 ± 0.4 Ma.*

**Trab** Autobrecciated rhyolite—*Autobrecciated facies of the rhyolite of Silver Peak.*

**Tst** Stratified tuff—*Moderately well-bedded volcanic sandstone containing clasts of pumice, volcanic rock fragments, and crystal fragments. Locally underlies the rhyolite of Silver Peak. Thickness unknown but probably less than 100 feet (30 m).*

**Tnv** Volcaniclastic rocks of Newcastle Reservoir—*Brick-red, moderately well-bedded volcaniclastic conglomerate and sandstone. Clasts composed of Racer Canyon Tuff, Harmony Hills Tuff, a variety of volcanic rocks, and lesser limestone, chert, and quartzite. Hematitic matrix is ubiquitous. Complete section not observed, but exposed thicknesses range from 300 to 1200 feet (90 to 365 m). Equivalent to the "Mine series" of Siders (1985a).*

**Tr** Racer Canyon Tuff—*Weakly to moderately welded, rhyolitic ash-flow tuff of whitish, gray, or pink color. Contains 30 to 35 percent crystals of quartz, plagioclase, sanidine, biotite, and minor Fe-Ti oxides, hornblende, and sphene. Lithic fragments are sparse. Thickness ranges from 300 to 1100 feet (90 to 330 m). Dated about 19 Ma.*

**Tri** Tuffaceous sandstone—*Bedded quartz-rich tuffaceous sandstone that locally occurs near the top of the Racer Canyon Tuff.*

**Tv** Volcaniclastic rocks—*Dark-colored, poorly sorted, crudely-bedded, cobble-rich, volcaniclastic mudflow breccia with local sandstone interbeds. Clasts composed dominantly of andesite and Harmony Hills Tuff. Unit is widely distributed and about 100 feet (30 m) thick.*

**Th** Harmony Hills Tuff—*Purplish, red, or brown (where altered) to light tan (where fresh), moderately welded, dacitic, crystal-rich ash-flow tuff. Contains about 50 percent crystals of plagioclase, quartz, biotite, amphibole, and Fe-Ti oxides. Thickness ranges from 200 to 400 feet (60 to 120 m). Dated about 21 Ma.*

**Tcc** Condor Canyon Formation—*Consists of densely-welded, rhyolitic to rhyodacitic vitric-crystal ash-flow tuffs and local andesite mudflow breccia. Contains two widely-distributed ash-flow tuffs, the upper Bauers Tuff (dated at 23 Ma) and the lower Swett Tuff (dated at 24 Ma) Members. Both tuffs contain distinctive flattened lenticules and about 15 percent crystals of plagioclase, iotite, and miner Fe-Ti oxides The Bauers Tuff ranges in thickness from 200 to 600 feet (60 to 180 m) and the Swett Tuff is less than 100 feet (30 m) thick.*

**Tccv** Volcaniclastic rocks of the Condor Canyon Formation—*Andesitic volcaniclastic horizon separating the Bauers and Swett Tuff Members throughout most of the district. Consists of volcanic mudflow breccia containing pebble- to boulder-sized clasts of andesite. Approximately 30 to 70 feet (9 to 20 m) thick.*

**Tl** Leach Canyon Tuff—*Pale cream to gray, moderately welded, ash-flow tuff containing 20 to 30 percent crystals of quartz, plagioclase, sanidine, and minor biotite and opaques. Contains conspicuous reddish lithic fragments. Table Butte and Narrows Members not distinguished. Thickness is about 500 feet (150 m). Dated about 25 Ma.*

**Ti** Isom Formation—*Dark-brown, densely welded, crystal-poor ash-flow tuff with distinctive, light-gray flattened lenticules. Contains sparse crystals of plagioclase, minor clinopyroxene and Fe-Ti oxides. Consists of two members, the upper Hole-in-the-Wall Tuff and lower Baldhills Tuff. Total thickness ranges from 500 to 1200 feet (90 to 360 m).*

**Tc** Claron Formation—*Composed of fluvial and lacustrine shale, siltstone, sandstone, limestone, and conglomerate. Lower portion dominated by red siltstone, sandstone, and conglomerate. Upper portion is mostly light-gray to mottled, freshwater limestone (with sparse leaf fossils), limestone-clast conglomerate, and lesser sandstone. Thickness ranges from 500 to 950 feet (150 to 290 m).*

**Kis** Iron Springs Formation—*Fluvial and lacustrine, light- to dark-brown, thin- to thick-bedded, continental sandstone and pebble- to cobble-conglomerate, with lesser interbedded siltstone, shale, and limestone. Base of unit includes a thin, discontinuous, basal conglomerate containing abundant quartzite clasts. Thickness ranges from about 1050 to 3600 feet (320 to 1100 m).*

**Jcb** Upper banded member of Carmel Formation—*Alternating bands of gray and maroon shale and siltstone. Between 0 and 100 feet (0 to 30 m) thick.*

**Jch** Homestake Limestone Member of the Carmel Formation—*Resistant, massive to thick-bedded, blue-gray limestone containing sparse invertebrate fossils. Upper portion is a thin-bedded, argillaceous lime stone. Base is not exposed in the quadrangle. A minimum thickness of 160 feet (50 m) is indicated.*

### CONTACT

Dashed where approximate; dotted where inferred

### FAULTS

Dashed where approximate; queried where uncertain; dotted where covered

Normal Fault

Bar and ball on downthrown side; dip indicated by arrow

Inferred Thrust Fault (on cross sections)

Gravity Slide Block
Dashed where inferred

### STRIKE AND DIP OF BEDDING AND ASH-FLOW TUFF LAYERING

10 Inclined — Vertical

### STRIKE AND DIP OF JOINTS

15 Inclined — Vertical

### STRIKE AND DIP OF SLICKENSIDES

15 Inclined; approximate plunge of grooves indicated

10 Horizontal; dip of surface indicated

### VEIN

78 Dip indicated by arrow

### MINE WORKINGS

adit — shaft — prospect — trench

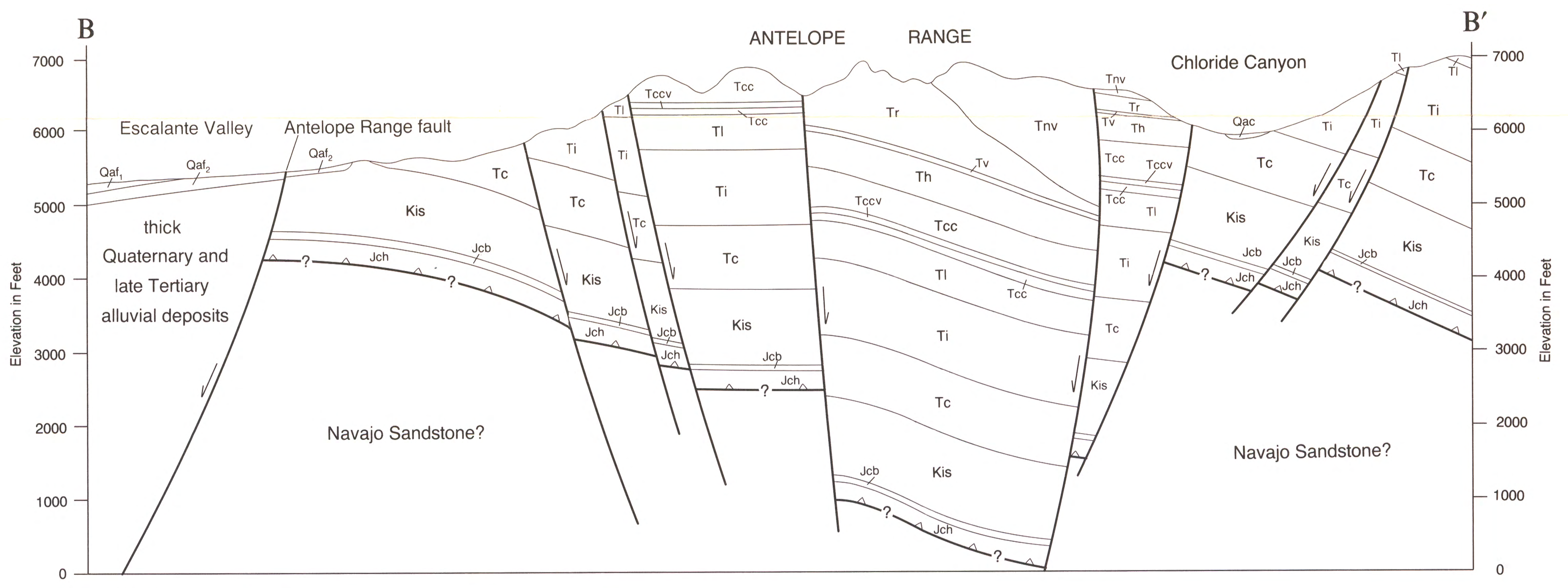


### CORRELATION OF MAP UNITS

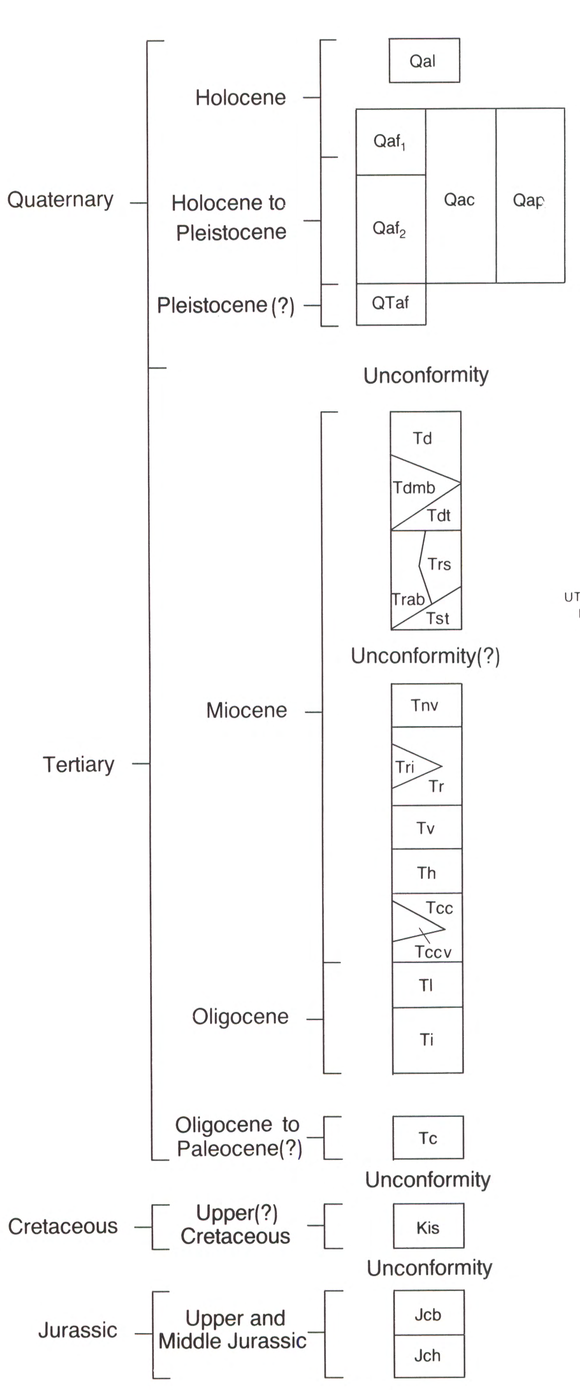


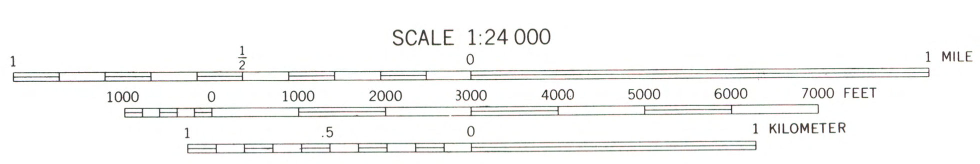


CONTOUR INTERVAL 20 FEET
NATIONAL GEODETIC VERTICAL DATUM OF 1929

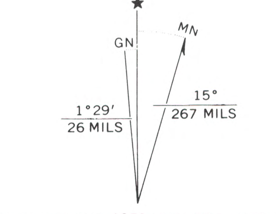


UTM GRID AND 1978 MAGNETIC NORTH DECLINATION AT CENTER OF SHEET

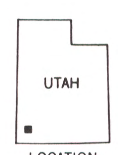


LOCATION

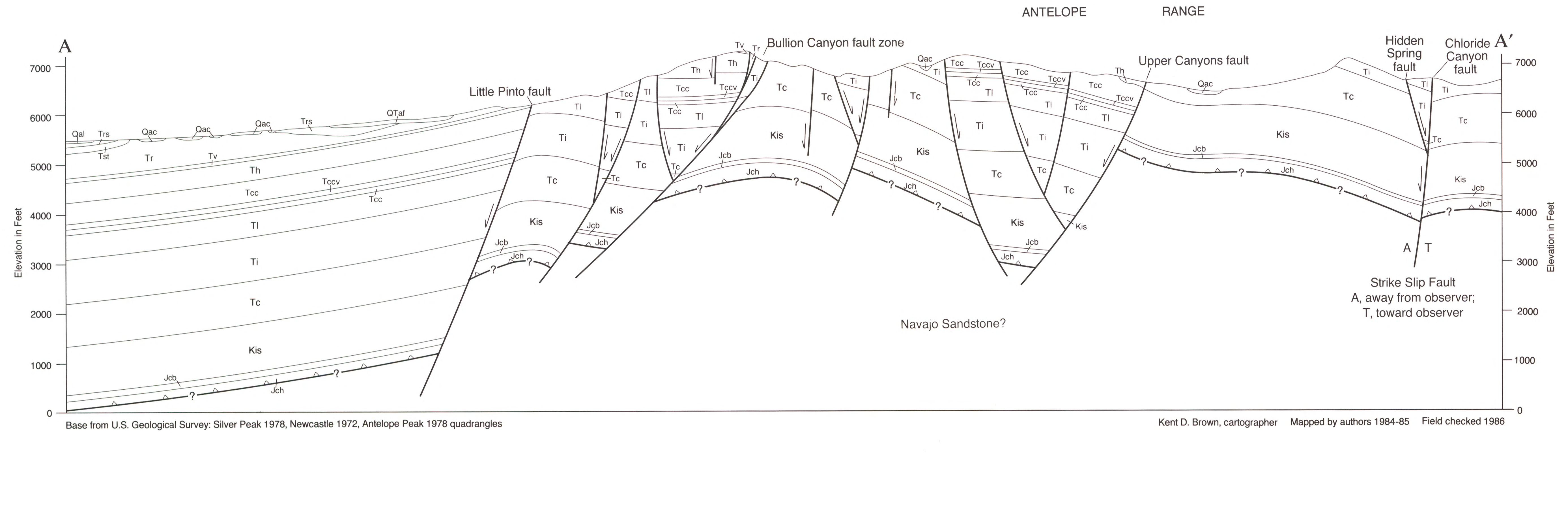


Base from U.S. Geological Survey: Silver Peak 1978, Newcastle 1972, Antelope Peak 1978 quadrangles

Kent D. Brown, cartographer    Mapped by authors 1984-85    Field checked 1986

STATE OF UTAH
DEPARTMENT OF NATURAL RESOURCES
UTAH GEOLOGICAL AND MINERAL SURVEY



# HYDROTHERMAL ALTERATION MAP OF THE ANTELOPE RANGE MINING DISTRICT, IRON COUNTY, UTAH

by
Michael A. Shubat[1] and W. Skip McIntosh[2]
[1]Utah Geological and Mineral Survey
[2]Colorado State University, Fort Collins, Colorado

1988

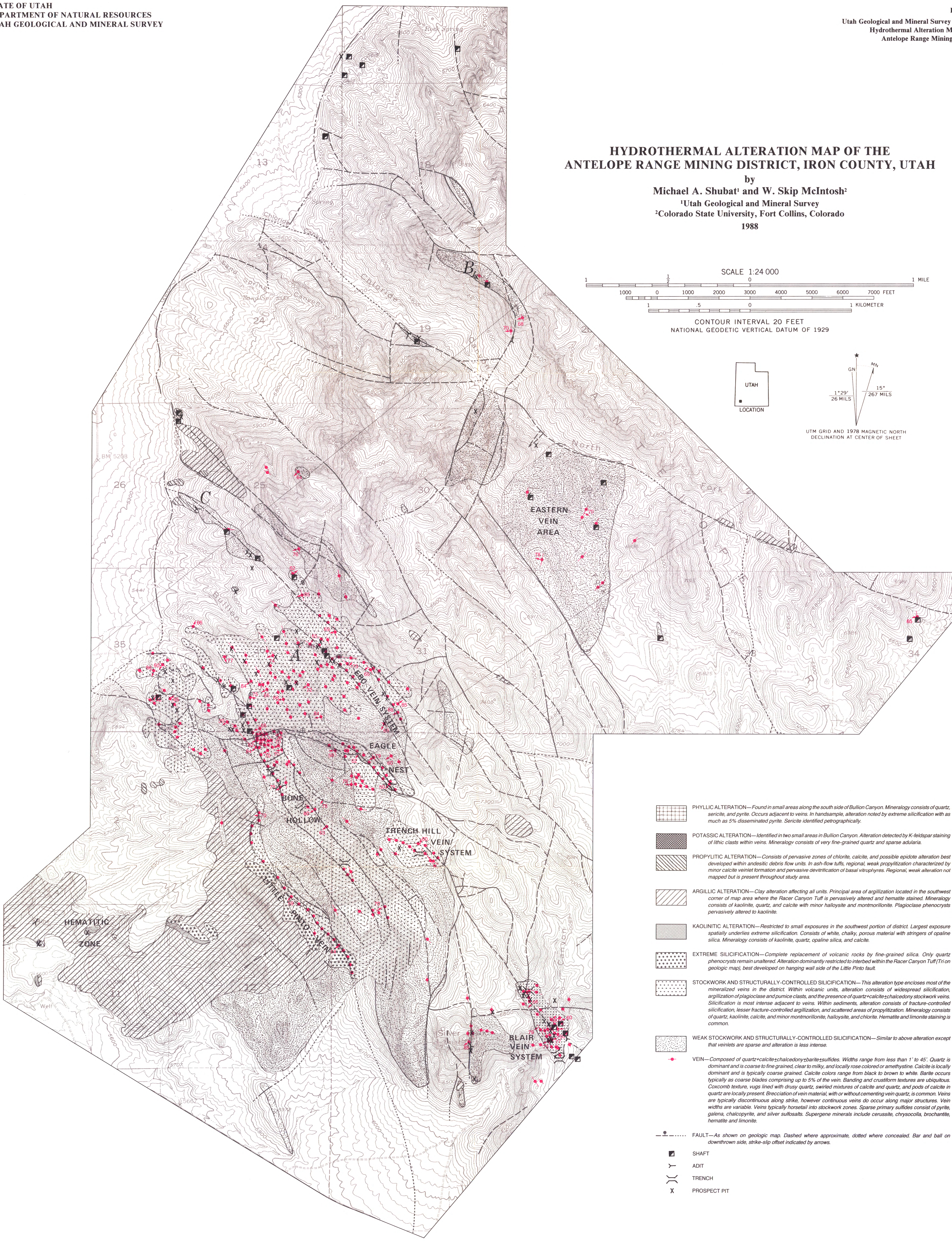


PHYLLIC ALTERATION—*Found in small areas along the south side of Bullion Canyon. Mineralogy consists of quartz, sericite, and pyrite. Occurs adjacent to veins. In handsample, alteration noted by extreme silicification with as much as 5% disseminated pyrite. Sericite identified petrographically.*

POTASSIC ALTERATION—*Identified in two small areas in Bullion Canyon. Alteration detected by K-feldspar staining of lithic clasts within veins. Mineralogy consists of very fine-grained quartz and sparse adularia.*

PROPYLITIC ALTERATION—*Consists of pervasive zones of chlorite, calcite, and possible epidote alteration best developed within andesitic debris flow units. In ash-flow tuffs, regional, weak propylitization characterized by minor calcite veinlet formation and pervasive devitrification of basal vitrophyres. Regional, weak alteration not mapped but is present throughout study area.*

ARGILLIC ALTERATION—*Clay alteration affecting all units. Principal area of argillization located in the southwest corner of map area where the Racer Canyon Tuff is pervasively altered and hematite stained. Mineralogy consists of kaolinite, quartz, and calcite with minor halloysite and montmorillonite. Plagioclase phenocrysts pervasively altered to kaolinite.*

KAOLINITIC ALTERATION—*Restricted to small exposures in the southwest portion of district. Largest exposure spatially underlies extreme silicification. Consists of white, chalky, porous material with stringers of opaline silica. Mineralogy consists of kaolinite, quartz, opaline silica, and calcite.*

EXTREME SILICIFICATION—*Complete replacement of volcanic rocks by fine-grained silica. Only quartz phenocrysts remain unaltered. Alteration dominantly restricted to interbed within the Racer Canyon Tuff (Tri on geologic map), best developed on hanging wall side of the Little Pinto fault.*

STOCKWORK AND STRUCTURALLY-CONTROLLED SILICIFICATION—*This alteration type encloses most of the mineralized veins in the district. Within volcanic units, alteration consists of widespread silicification, argillization of plagioclase and pumice clasts, and the presence of quartz+calcite±chalcedony stockwork veins. Silicification is most intense adjacent to veins. Within sediments, alteration consists of fracture-controlled silicification, lesser fracture-controlled argillization, and scattered areas of propylitization. Mineralogy consists of quartz, kaolinite, calcite, and minor montmorillonite, halloysite, and chlorite. Hematite and limonite staining is common.*

WEAK STOCKWORK AND STRUCTURALLY-CONTROLLED SILICIFICATION—*Similar to above alteration except that veinlets are sparse and alteration is less intense.*

VEIN—*Composed of quartz+calcite±chalcedony±barite±sulfides. Widths range from less than 1' to 45'. Quartz is dominant and is coarse to fine grained, clear to milky, and locally rose colored or amethystine. Calcite is locally dominant and is typically coarse grained. Calcite colors range from black to brown to white. Barite occurs typically as coarse blades comprising up to 5% of the vein. Banding and crustiform textures are ubiquitous. Coxcomb texture, vugs lined with drusy quartz, swirled mixtures of calcite and quartz, and pods of calcite in quartz are locally present. Brecciation of vein material, with or without cementing vein quartz, is common. Veins are typically discontinuous along strike, however continuous veins do occur along major structures. Vein widths are variable. Veins typically horsetail into stockwork zones. Sparse primary sulfides consist of pyrite, galena, chalcopyrite, and silver sulfosalts. Supergene minerals include cerussite, chrysocolla, brochantite, hematite and limonite.*

FAULT—*As shown on geologic map. Dashed where approximate, dotted where concealed. Bar and ball on downthrown side, strike-slip offset indicated by arrows.*

SHAFT

ADIT

TRENCH

PROSPECT PIT